AD-A093 400 TEXAS UNIV AT AUSTIN GEOTECHNICAL ENGINEERING CENTER F/G 8/13
DEVELOPMENT OF A LARGE-SCALE TRIAXIAL TESTING DEVICE FOR WAVE P--ETC(U)
NOV 80 K H STOKOE, D P KNOX, J M ROESSET AFOSR-80-0031
UNCLASSIFIED GR80-10 AFOSR-TR-80-1319 NL

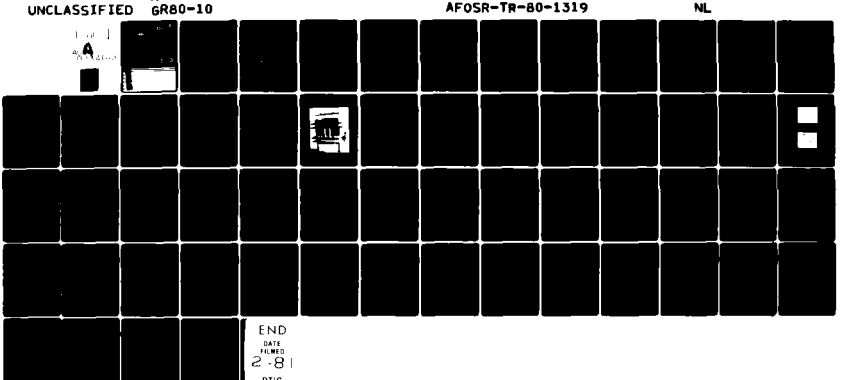

END
DATE FILMED
2-81
DTIC

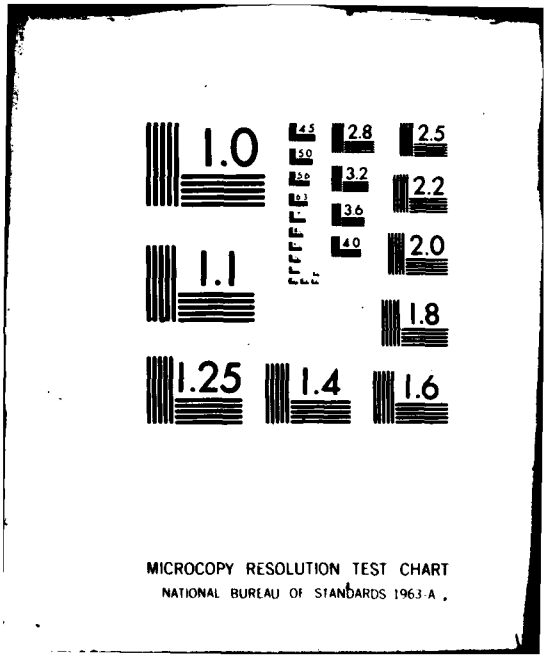
1.0
1.1
1.25
1.4
1.6
1.8
2.0
2.2
2.5
2.8
3.2
3.6
4.0
4.5
5.0
MICROCOPY RESOLUTION TEST CHART
NATIONAL BUREAU OF STANDARDS 1963-A

AFOSR-TR. 80-1319

LEVEL II 3

DEVELOPMENT OF A LARGE-SCALE TRIAXIAL [redacted] TESTING DEVICE FOR WAVE PROPAGATION STUDIES

K. H. Stokoe, J. M. Roesset
D. P. Knox, S. E. Kopperman,
and C. Suddhiprakarn

a report on research
sponsored by
United States Air Force
Office of Scientific Research
Bolling Air Force Base

SECURITY CLASSIFICATION OF THIS PAGE (When Data Entered) UNCLASSIFIED

REPORT DOCUMENTATION PAGE

READ INSTRUCTIONS BEFORE COMPLETING FORM

1. REPORT NUMBER: AFOSR-TR-80-1319	2. GOVT ACCESSION NO.: AD A093400
3. RECIPIENT'S CATALOG NUMBER	
4. TITLE (and Subtitle): DEVELOPMENT OF A LARGE SCALE TRIAXIAL TESTING DEVICE FOR WAVE PROPAGATION STUDIES.	5. TYPE OF REPORT & PERIOD COVERED: Interim rept.
6. PERFORMING ORG. REPORT NUMBER	
7. AUTHOR(s): K. H. STOKOE, J. M. ROESSET, C. SUDDHIPRAKARN, D. P. KNOX, S. E. KOPPERMAN	8. CONTRACT OR GRANT NUMBER(s): AFOSR-80-0031
9. PERFORMING ORGANIZATION NAME AND ADDRESS: UNIVERSITY OF TEXAS/AUSTIN, CIVIL ENGINEERING DEPARTMENT, AUSTIN TEXAS 78712	10. PROGRAM ELEMENT, PROJECT, TASK AREA & WORK UNIT NUMBERS: 61102F, 2307/C1
11. CONTROLLING OFFICE NAME AND ADDRESS: AIR FORCE OFFICE OF SCIENTIFIC RESEARCH/NA, BOLLING AFB DC 20332	12. REPORT DATE: NOV 1980
	13. NUMBER OF PAGES: 50
14. MONITORING AGENCY NAME & ADDRESS (if different from Controlling Office): GRSD-TR	15. SECURITY CLASS. (of this report): UNCLASSIFIED
	15a. DECLASSIFICATION/DOWNGRADING SCHEDULE

16. DISTRIBUTION STATEMENT (of this Report)

Approved for public release; distribution unlimited

17. DISTRIBUTION STATEMENT (of the abstract entered in Block 20, if different from Report)

18. SUPPLEMENTARY NOTES

19. KEY WORDS (Continue on reverse side if necessary and identify by block number)

SOIL MECHANICS
GEOTECHNICAL
TRIAXIAL
SEISMIC
WAVE PROPAGATION
SHEAR MODULUS
SOIL DYNAMICS

20. ABSTRACT (Continue on reverse side if necessary and identify by block number)

Experimental and analytical studies have been undertaken to investigate the effects of the 3-D state of stress on the charactertistics of seismic waves in soil. The initial experimental studies involve testing instrumented cubes of dry sand where the principal normal stresses are controlled independently. Compression (P) and shear (S) waves are generated on the sides of the sand cube and propagate through the body of the sand. Wave lengths and frequencies are in the range of 0.5 to 2.0 ft and 300 to 1000 Hz, respectively. Accelerometers embedded in the sand body are used to monitor wave arrivals and amplitudes

DD FORM 1 JAN 73 1473 EDITION OF 1 NOV 65 IS OBSOLETE

412111

SECURITY CLASSIFICATION OF THIS PAGE (When Data Entered) UNCLASSIFIED

from which propagation velocities and attenuation under the various states of stress are calculated. The design and fabrication of the experimental facilities are presented. A metal-walled cube has been constructed with rubber membranes to apply confining pressures. In the center of each wall are excitation ports where impulses are applied to excite P- and S- waves in the sand at shearing strains below 0.01 percent. Analytical studies have concentrated on evaluating the disturbance created by an accelerometer, considered as a rigid body, on the wave front travelling through the soil. Two different approaches have been considered: the boundary integral equation method and a finite element formulation. Results are presented. The work described herein represents the first step in a long-range program to investigate experimentally the dynamic behavior of soils under arbitrary states of stresses and to study analytically the most appropriate procedures to model this behavior.

DEVELOPMENT OF A LARGE-SCALE TRIAXIAL TESTING DEVICE FOR WAVE PROPAGATION STUDIES

K.H. Stokoe, J.M. Roesset
D.P. Knox, S.E. Kopperman
and C. Suddhiprakarn

a report on research
sponsored by
United States Air Force
Office of Scientific Research
Bolling Air Force Base

November, 1980

Geotechnical Engineering Report GR80-10
Geotechnical Engineering Center
Civil Engineering Department
The University of Texas at Austin
Austin, Texas

ACKNOWLEDGEMENTS

This study was supported by the U.S. Air Force Office of Scientific Research (AFOSR), Bolling Air Force Base, Washington, D.C. under Grant AFOSR-80-0031. Major John J. Allen was the program manager. The writers wish to thank AFOSR and Major Allen for their support. The assistance of Mr. W. Howell in the structural design of the triaxial cube is appreciated. The allocation of work space and the assistance and cooperation of personnel at the Ferguson Structural Research Laboratory is sincerely appreciated.

TABLE OF CONTENTS

		Page
ACKNOWLEDGEMENTS		ii
LIST OF FIGURES		iv
1.0	INTRODUCTION	1
2.0	TRIAXIAL CUBE	2
	2.1 Structure of Cube	4
	2.2 Loading System	9
	2.3 Excitation Ports	15
	2.4 Monitoring and Recording Systems	19
	2.5 Sand Placement	22
3.0	SAND USED IN INITIAL TESTING	24
	3.1 Dynamic Testing	26
	3.2 Low-Amplitude Dynamic Properties	26
	3.3 Intermediate-Amplitude Dynamic Properties	28
4.0	ANALYTICAL STUDIES	31
	4.1 Mathematical Model	33
	4.2 Results of Finite Element Studies	34
	4.3 Conclusions	46
5.0	SUMMARY	46
6.0	REFERENCES	50

LIST OF FIGURES

Figure Number		Page
1	Schematic of Triaxial Cube and Associated Equipment	3
2	Cut Away Isometric View of Triaxial Cube Showing Top Reinforcement Details	5
3	Isometric View of Triaxial Cube Showing Side Reinforcement Details	6
4	Cross-Sectional View Along Central Horizontal Plane in Triaxial Cube	7
5	Cross-Sectional View Along Central Vertical Plane in Triaxial Cube	8
6	Completed Cube Structure	10
7	Construction of Membranes	12
8	Schematic of Air/Water System Used to Pressurize the Membranes	14
9	Excitation Hammer in Each Port of Triaxial Cube	16
10	Typical Travel Time Records for Surface Source and Embedded Receivers	18
11	Schematic of Monitoring and Recording Systems	20
12	Isometric View of 3-D Accelerometer Package	21
13	Sand Placement System	23
14	Grain Size Analysis of Washed Mortar Sand	25
15	Variation in Low-Amplitude Shear Modulus with Confining Pressure	27
16	Variation in Low-Amplitude Damping Ratio with Confining Pressure	29
17	Variation in Shear Modulus with Shearing Strain	30

Figure Number		Page
18	Variation in Material Damping Ratio with Shearing Strain	32
19	Acceleration-Time History of Left Corner of Soil Element in a Sand Mass without Rigid Inclusions	35
20	Acceleration-Time History of Right Corner of Soil Element in a Sand Mass without Rigid Inclusions	36
21	Acceleration-Time History of Left Corner of Rigid Inclusion in a Sand Mass	38
22	Acceleration-Time History of Right Corner of Rigid Inclusion in a Sand Mass	39
23	Acceleration-Time History of Center of Rigid Inclusion in a Sand Mass	40
24	Angular Acceleration-Time History of Center of Rigid Inclusion in a Sand Mass	41
25	Acceleration-Time History of Left Corner of Central Inclusion in a Sand Mass with Three Rigid Inclusions	42
26	Acceleration-Time History of Right Corner of Central Inclusion in a Sand Mass with Three Rigid Inclusions	43
27	Acceleration-Time History of Center of Central Inclusion in a Sand Mass with Three Rigid Inclusions	44
28	Angular Acceleration-Time History of Center of Central Inclusion in a Sand Mass with Three Rigid Inclusions	45
29	Acceleration-Time History of Left Corner of Soil Element in a Sand Mass without Rigid Inclusions for 3-D Analysis	47
30	Acceleration-Time History of Right Corner of Soil Element in a Sand Mass without Rigid Inclusions for 3-D Analysis	48

1.0 INTRODUCTION

Very little is known about the three-dimensional (3-D) state of stress on the velocity and attenuation of compression and shear waves in the soil. Geologic materials are typically analyzed assuming they are homogeneous and isotropic. The behavior of these materials under 3-D states of stress is, however, of fundamental importance in the prediction of ground response and soil-structure interaction during all types of dynamic loadings ranging from small-strain machine loading to high-strain blast loading. In addition, understanding of this basic wave behavior in soil has the potential to be used: 1. to improve in situ seismic techniques used to investigate soil sites, 2. to determine the in situ structure of soil, 3. to estimate the initial state of stress in soil, and 4. to improve soil models used in computer codes for the analysis of the dynamic soil response.

A basic research program combining both experimental and analytical studies has been undertaken to investigate the effects of the 3-D state of stress on the characteristics of seismic waves in soil. The initial experimental studies involve testing instrumented cubes of dry sand. The sand cubes are about 7 ft on a side and are loaded with principal effective normal stresses ($\bar{\sigma}_1$, $\bar{\sigma}_2$, and $\bar{\sigma}_3$) parallel to the three axes of the cube. The principal normal stresses are controlled independently so that a true triaxial state of stress can be applied ($\bar{\sigma}_1 > \bar{\sigma}_2 > \bar{\sigma}_3$). Compression (P) and shear (S) waves are generated on the sides of the sand cube and propagate through the body of the sand. Wave lengths and frequencies are in the range of 0.5 to 2.0 ft and 300 to 1000 Hz, respectively. Accelerometers embedded in the sand body are used to monitor wave arrivals and amplitudes from which propagation velocities and attenuation under the various states of stress are calculated.

The design and fabrication of the experimental facilities used in this research program are presented in Section 2 of this report. Basically, a metal-walled cube with interior dimensions of 7 ft on a side has been constructed. Rubber membranes attached to the inside walls are used to apply confining pressures. In the center of each wall, excitation ports have been constructed through which mechanical coupling is made

made between the sand in the cube and a mechanical exciter outside the cube. Impulses applied at the excitation ports are used to excite P- and S-waves in the sand at shearing strains below 0.01 percent.

The analytical studies during the initial work have concentrated on evaluating the disturbance created by an accelerometer, considered as a rigid body, on the wave front travelling through the soil. Two different approaches have been considered: use of the boundary integral equation method and a finite element formulation. The results of these studies are presented in Section 4.

The work described herein represents the first step in a long-range program to investigate experimentally the dynamic behavior of soils under arbitrary states of stresses and to study analytically the most appropriate procedures to model this behavior.

2.0 TRIAXIAL CUBE

Much of the effort in the project for the first year has been directed toward the design and fabrication of the triaxial cube and associated equipment. This work has been done to prepare for initial wave propagation testing with dry sand. The cube is a steel structure with interior dimensions of 7 ft on a side. The associated equipment is used to: 1. place the sand, 2. pressurize the cube, 3. excite compression and shear waves in the sand, and 4. monitor and record these waves. A schematic diagram of the cube and associated equipment is shown in Fig. 1.

As of 30 September 1980, the cube is approximately 95 percent completed and all of the associated equipment has either been purchased or designed and fabricated. Of the associated equipment, the pressurizing system has been fabricated and is currently being pretested, the electronics system is in the process of being built with both the source hammers and one of the digital oscilloscopes already in place, and the sand placement system is ready for use. A discussion of the cube and these systems is presented in the following sections.

The cube and associated equipment are located at the Ferguson Structural Research Laboratory at the Balcones Research Center of The University of Texas at Austin.

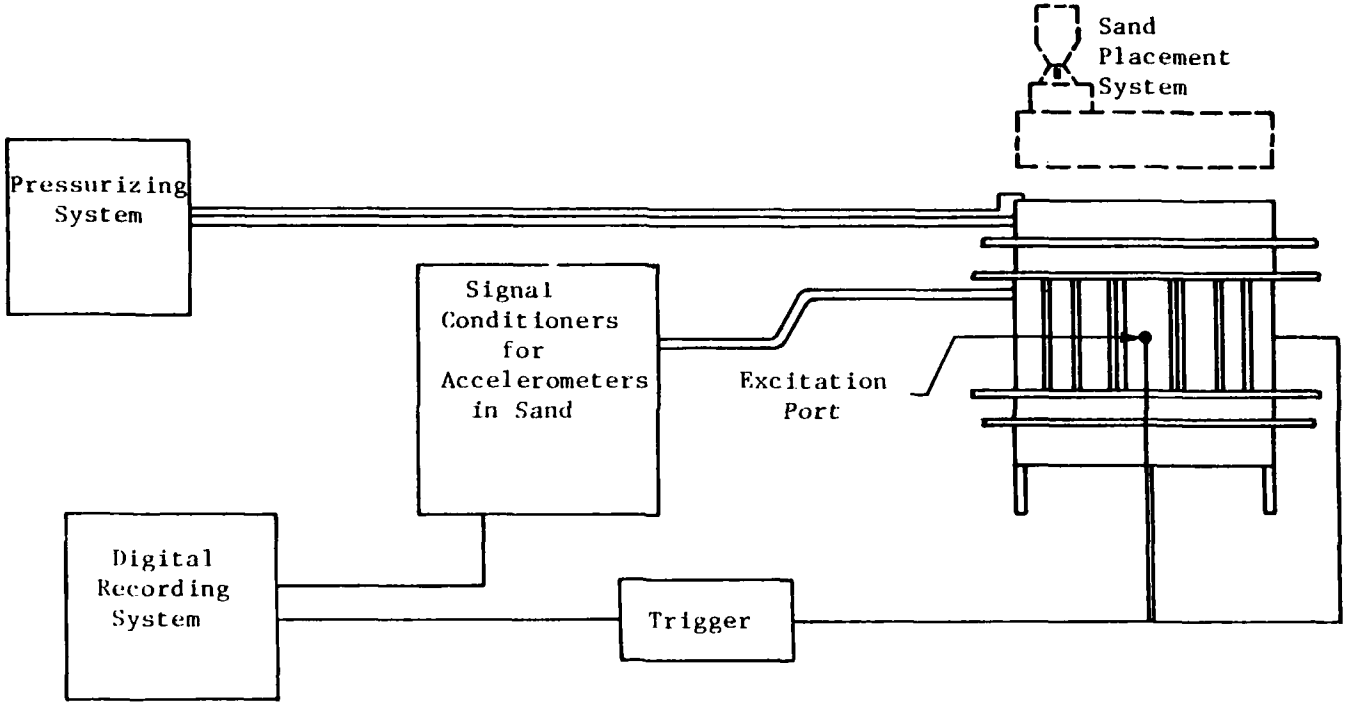

Fig. 1 - Schematic of Triaxial Cube and Associated Equipment

2.1 Structure of Cube

Initially it was envisioned that the cube would be constructed of plain steel plates approximately 7-ft square. However, subsequent calculations showed that a plate thickness of about 12 in. would be required to restrict the bending of the plates to an acceptable value under a desired maximum working pressure of 50 psi. A compromise between reduced plate thickness and substantial reinforcement was decided upon to reduce the cost of the steel, with the added benefit of lowering the total weight of the structure. In the final design, 0.038-in. thick, mild steel plates were employed to form all six sides of the cube. These steel plates were reinforced with lateral and longitudinal bracing so that the cube could have a working pressure of 50 psi over any side.

The cube was designed to be built in three separate sections: 1. the bottom with four base legs, 2. the four sides, and 3. the top. These three sections were then bolted together to form the completed structure. In typical use, the four sides remain bolted to the bottom section and only the top is removed as the cube is filled or emptied of sand.

Both the top and bottom sections are similar in design except for the legs on the bottom section. Each section consists of a 7-ft square steel plate with reinforcement from large angles (L 8x8) to which 0.5-in. thick, steel plate sections are welded as shown in Fig. 2. The legs on the bottom section are included in the design to allow access to the bottom of the cube with its excitation port (see Section 2.3).

The four sides of the cube are constructed of 0.038-in. thick steel plates with angles and I-beam reinforcement. Steel angles (L 3½x3½ and L 6x6) are used as lateral reinforcement along the mid-section of the sides as shown in Fig. 3. These angles transfer the load to longitudinal, 14-in. I-beams (W 14x26) which form two continuous rings around the cube. In addition, there are two more longitudinal rings of 12-in. I-beams (W 12x16½) to restrict the bending of the outer edges of the steel plates. This reinforcement is shown in Figs. 4 and 5.

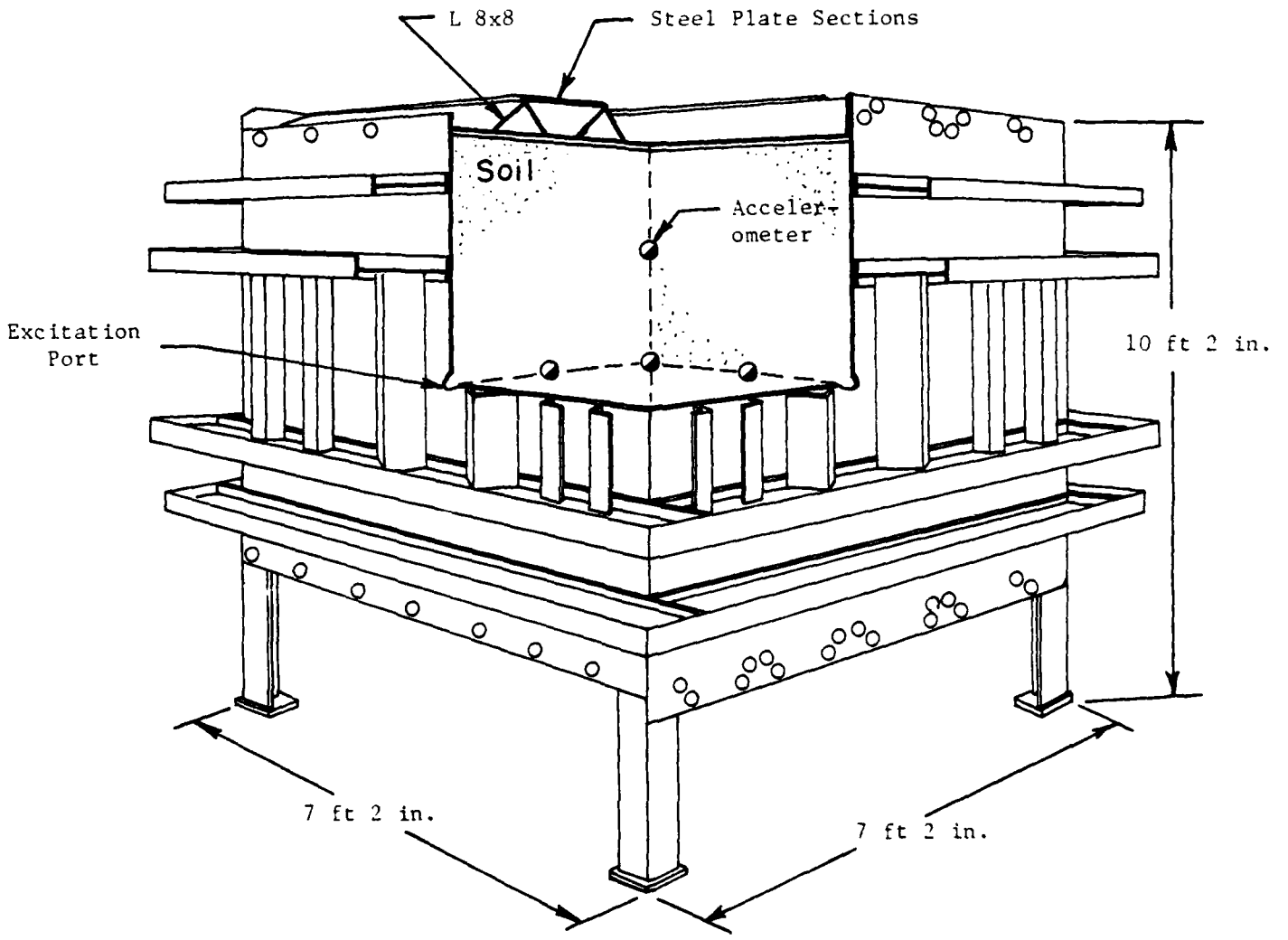

Fig. 2 - Cut Away Isometric View of Triaxial Cube
Showing Top Reinforcement Details

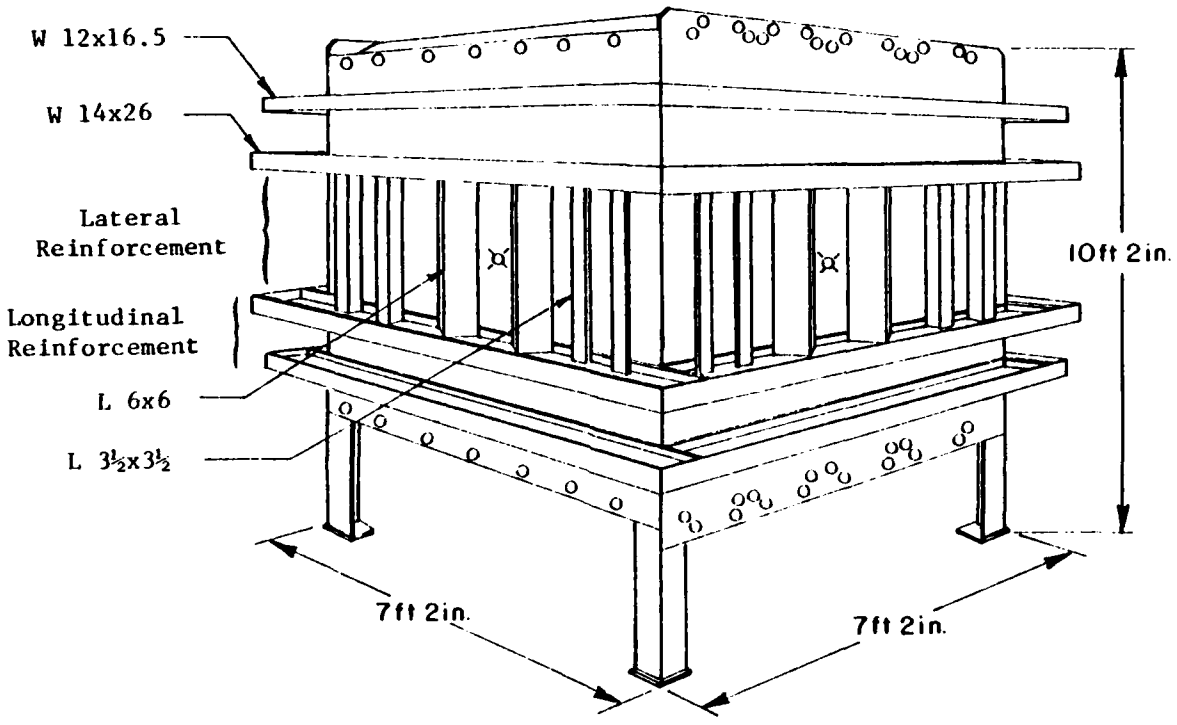

Note: See Figs. 4 and 5 for Cross-Sectional Detail Views

Fig. 3 - Isometric View of Triaxial Cube Showing Side Reinforcement Details

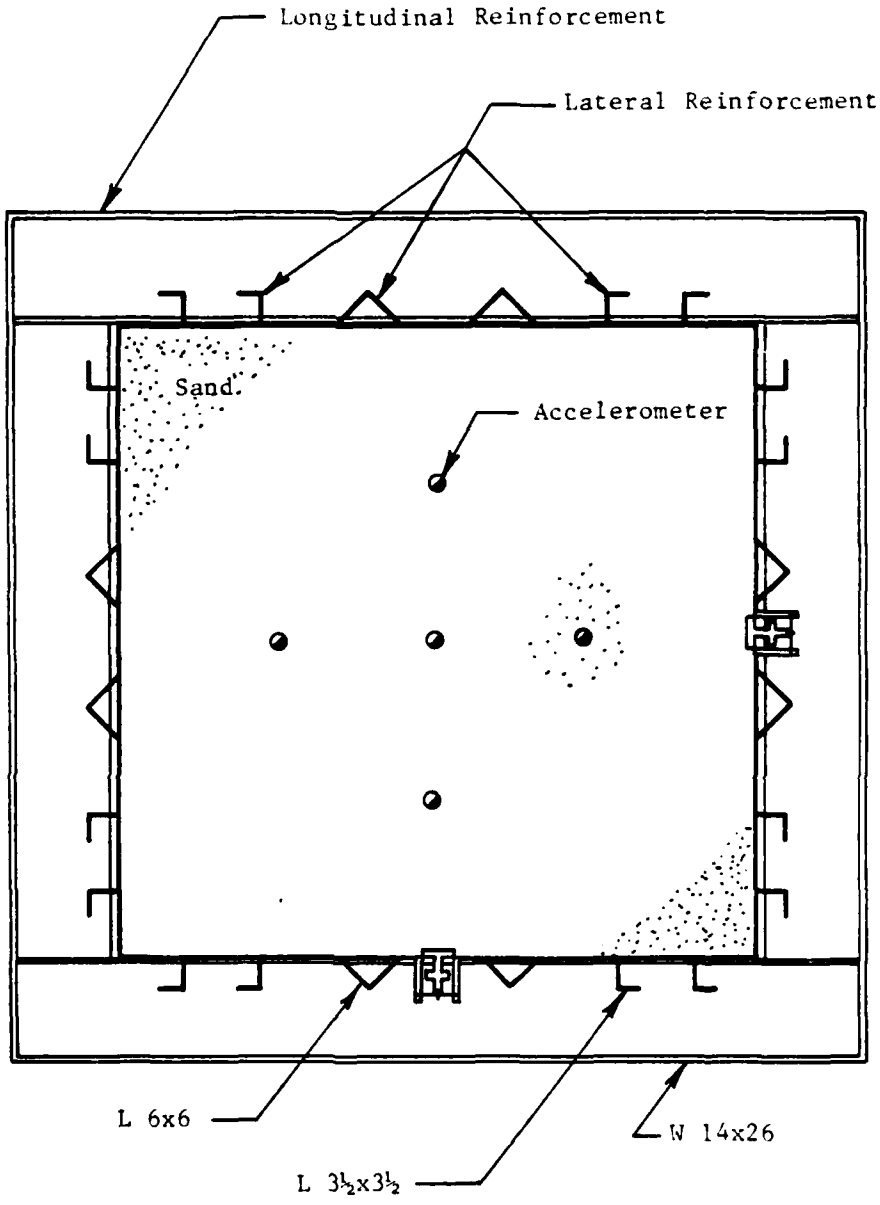

Fig. 4 - Cross-Sectional View Along Central Horizontal Plane in Triaxial Cube

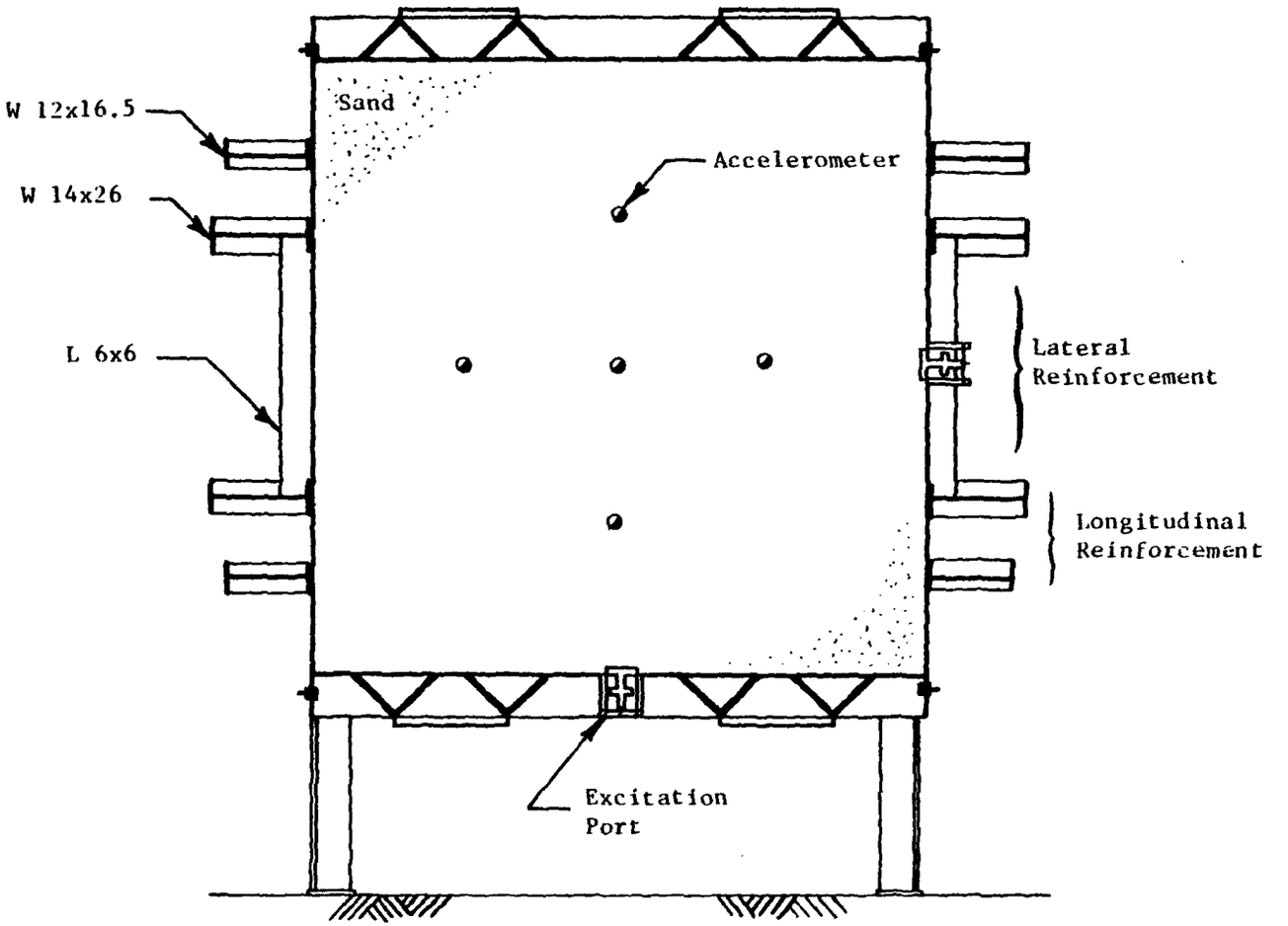

Fig. 5 - Cross-Sectional View Along Central Vertical Plane in Triaxial Cube

The procedure used in constructing the sides of the cube consisted of: 1. tack welding the reinforcement to the side plates, 2. bolting each side plate to the already completed bottom, 3. tack welding the four sides together while bolted to the bottom, and 4. final welding of the reinforcement to the side plates and final welding of the edges of the side plates together. This procedure was followed in order to reduce the possible deformation of the thin steel plates due to the welding heat. Initial tack welding secured the reinforcement to the side plates with a minimum of heat created in the plates. With the four sides bolted to the bottom, tack welding of the plates together ensured that the final shape would not deform considerably from the design shape.

The final design of the structure incorporates several desirable features. The cube has been designed as a free-standing structure without the need for any external support. In addition, lifting lugs are provided on the top section of the cube to permit movement of the cube whether full or empty with the 25-ton overhead crane at the Ferguson Laboratory. Further, excitation ports were fabraicted in each face of the cube to provide complete versatility in the location of wave generation. Also a steel ladder on rollers was constructed at the same height as the uppermost I-beam, approximately 9 ft above the ground, to permit easy access to the top of the cube and also to provide a safe working platform at the top of the cube.

At this time, the cube is completely fabricated and painted. The structure was painted two shades of blue on the outside, light blue on the steel plates and dark blue on the reinforcement. All of the inside was painted light blue. Only minor painting of the steel ladder remains to be done. Figure 6 shows the completed cube structure.

2.2 Loading System

Confining stresses are applied to the sand mass within the cube by membranes placed on the inside of the cube along the top and two adjacent sides. In this configuration, one membrane is used to apply

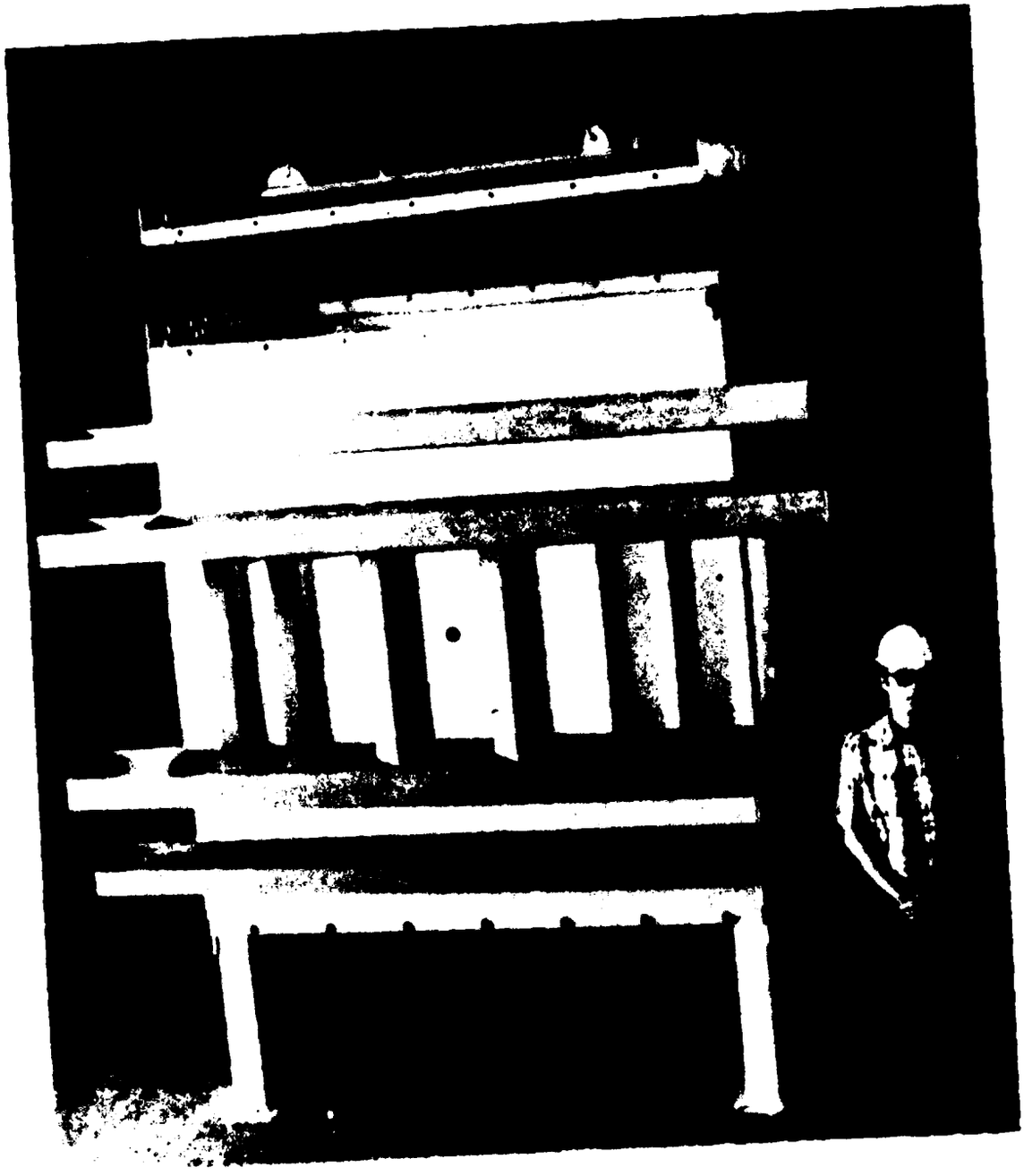

Fig. 6 - Completed Cube Structure

pressure along each of the three principal axes of the cube. The membranes are confined along their perimeter by steel ribs welded along the inside faces of the cube so that each membrane is isolated from the others and exerts a pressure only along its respective axis. This arrangement permits independent control of the pressure in each of the three principal directions. Loading conditions on the sand can then be of an isotropic ($\sigma_1 = \sigma_2 = \sigma_3$), anisotropic ($\sigma_1 \neq \sigma_2 = \sigma_3$), or true triaxial ($\sigma_1 \neq \sigma_2 \neq \sigma_3$) nature.

The loading system consists of membranes made of 0.063-in. thick Butyl rubber sheets. Each membrane is formed by bonding together two sheets of Butyl rubber, a smaller sheet cut to the size of the cube face against which it is to be palced, and a larger sheet cut to allow a 4-in. overlap splice along the perimeter edges of the smaller Butyl sheet. These two sheets are bonded together with cement to form a continuous lap seal around the perimeter of the smaller sheet. A sealant was placed inside the membrane along all lap-splice seams to form watertight seals between the two sheets. In addition, a sheet of filter fabric was placed between the rubber sheets in each membrane permitting water to permeate freely throughout the membrane. Water throughout the membrane will ensure that the pressure will be distributed equally and completely across the cube face in contact with the membrane. Figure 7 shows the construction of the membranes.

The procedure for membrane construction consisted of: 1. cutting and aligning the rubber sheets and filter fabric, 2. cleaning the sheets with a solvent, 3. applying the sealant with a caulking gun in a continuous bead along the inside fold of the intended overlap splice, and 4. placing the bonding cement on the rubber sections to be sealed and folding over and pressing together these rubber sections to form the splice seal.

The membranes are hydraulically loaded throughout the working pressure range of 0 to 50 psi. Hydraulic loading was selected from the safety point of view. Water under these pressures is safer than air because of the incompressibility of the water.

Pressurizing the membrane is accomplished through two inflow/outflow ports incorporated in opposite corners of each membrane. These ports

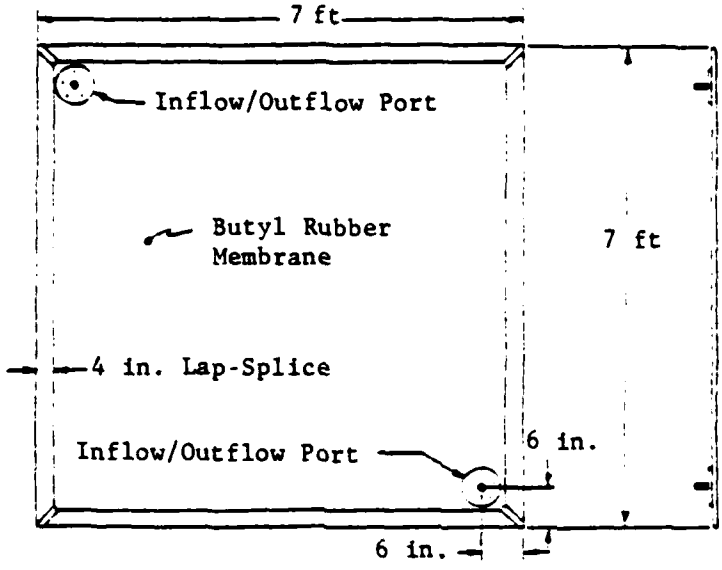

a. Typical Membrane with Inflow/Outflow Ports

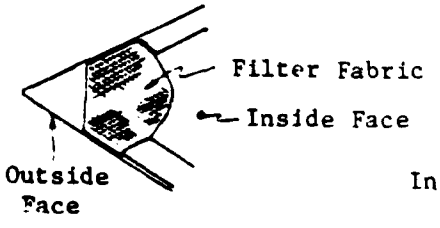

b. Detail of Membrane with Inner Filter Fabric

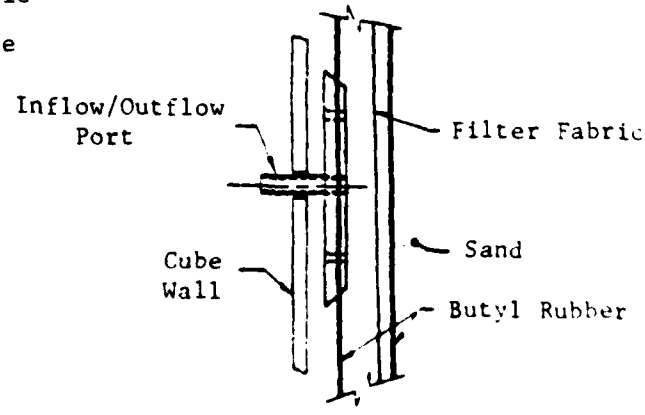

c. Expanded View of Inflow/Outflow Port

Fig. 7 - Construction of Membranes

provide a channel from the exterior pressure lines through the steel cube walls and into the membranes. The ports consist of a 4-in. long by 0.38 in. diameter pipe nipple passing through one of the Butyl sheets. This short pipe is screwed into two, 6-in. diameter steel plates between which is fastened the rubber sheet. These plates have a combined thickness of 0.5 in. Sealant is placed around the port and along the screwholes and connections to prevent any water leakage from the membranes. Once the sand is in place, the membranes are filled with water through the bottom port while air is expelled from the top port until the water level in the membrane reaches the top port.

Air pressure is used to pressurize the water in the membranes. This is done through a specially constructed panel board shown schematically in Fig. 8. Air pressure from the Balcones Research Center air supply (125 psi) enters a manifold in the panel board and is then independently controlled by three air regulators, one regulator for each membrane. The addition of an accurate Heise gauge into the panel board allows the air pressure to be accurately set with each air regulator and to be continuously monitored thereafter for each membrane. The regulated air pressure for each membrane passes to an air-water accumulator where the air pressure is transformed into water pressure. The water pressure is then directed toward a membrane outlet in the panel board to which a pressure line for the membrane is connected. The panel board can also be used to fill the membranes after the sand is in place. A water source is connected to the panel board and water is stored in the accumulator (up to 0.5 gallons). The water is then forced out of the accumulator and into the membrane with the use of air pressure.

At this time the loading system has been built. It is currently undergoing testing to determine how well the membranes are sealed. There have been continued leakage problems of water around the pipe nipple. However, it is now planned to prevent this leakage by: 1. coating the steel plates and surrounding rubber sheet with an adhesive sealant covered with a sheet of rubber, or 2. replacing the

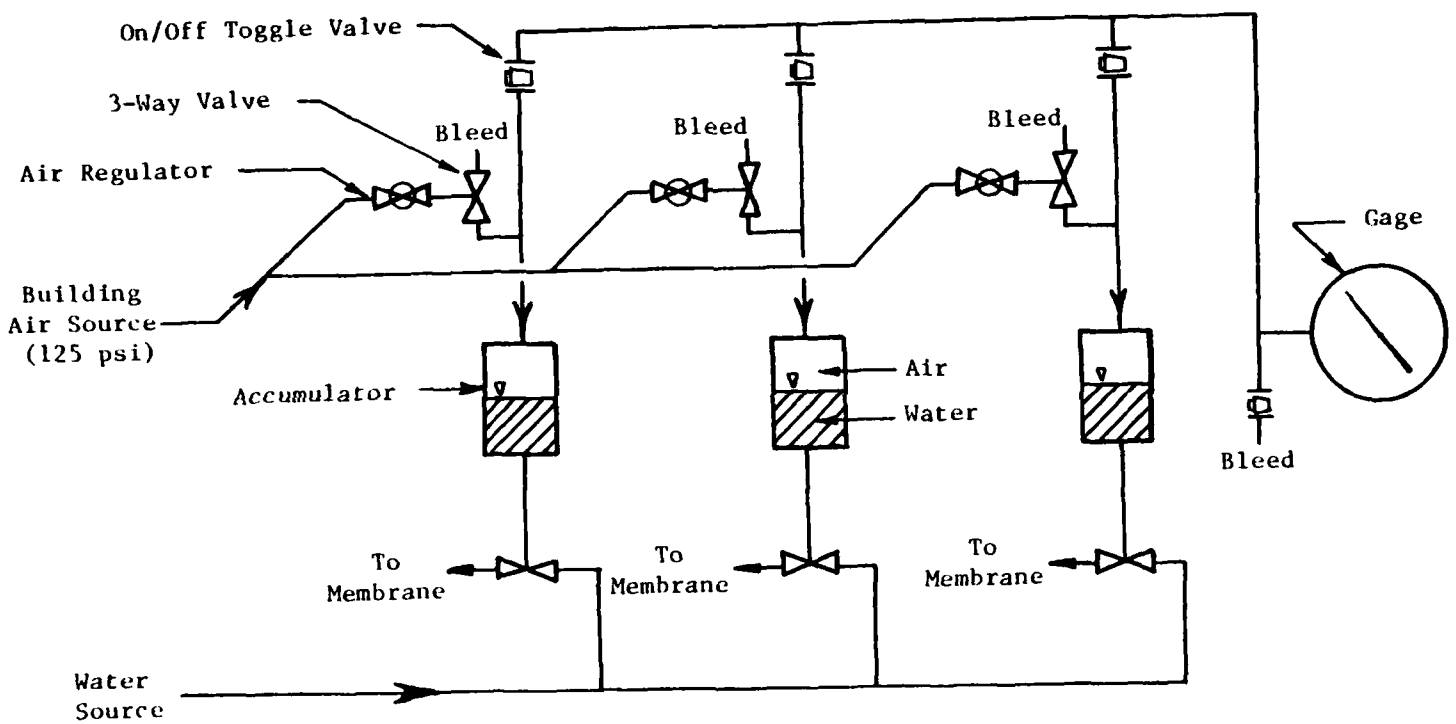

Fig. 8 - Schematic of Air/Water System Used to Pressurize the Membranes

present port design with one molded within a rubber covering. Presently both methods are being compared to see which offers the best solution to this leakage problem.

2.3 Excitation Ports

Since the objective of this research is to study the propagation characteristics of P- and S-waves through a soil mass, a mechanism for generating these waves at the soil boundaries is necessary. The ideal situation is a wave source in contact with the boundary of the soil mass inside the cube which is excitable from outside the cube. To achieve this goal, ports (i.e., holes in the cube walls) have been placed in the center of three mutually perpendicular sides of the cube: the bottom and two adjacent sides. At each port, an excitation system is attached which is composed of: 1. an excitation anvil, 2. an external frame, 3. an internal frame, 4. an adjustment screw, and 5. a hand held hammer. This system (*without the* hand-held hammer) is shown in Fig. 9.

The excitation port permits generation of P-waves or S-waves at the boundary of the soil mass by striking the anvil with the hand-held hammer. A 3-in. square plate at about the midlength of the shaft of the anvil is provided for the striking surface. Shear waves are generated in the soil by striking this plate either horizontally or vertically (parallel to the side of the cube). Compression waves are generated by striking the plate on the anvil in the direction of the axis of anvil (perpendicular to the side of the cube).

To perform properly, the base of the anvil which is in contact with the soil must maintain the same pressure against the soil as the surrounding face of the cube. This is accomplished by using the adjustment screw shown in Fig. 9 to push the anvil against the soil. The screw is threaded through a plate and bears against the anvil itself. The plate is part of an external frame which is bolted to the outside of the cube. The bolts holding the external frame on the outside are actually part of an internal frame which prevents soil displacement around the base of the anvil inside the cube when the anvil is excited.

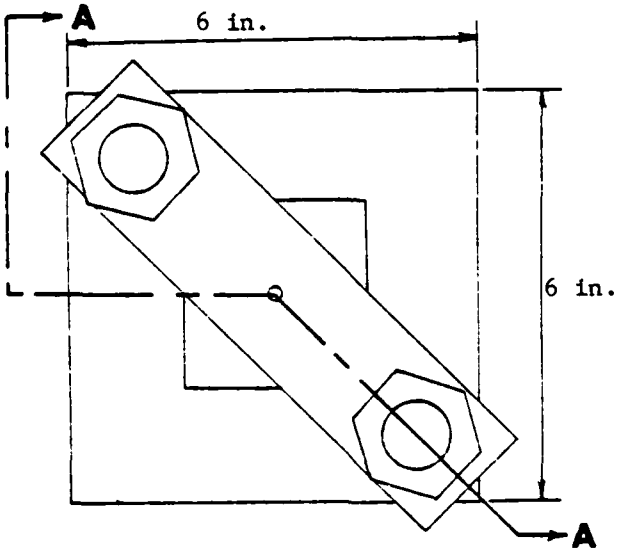

a. Top View

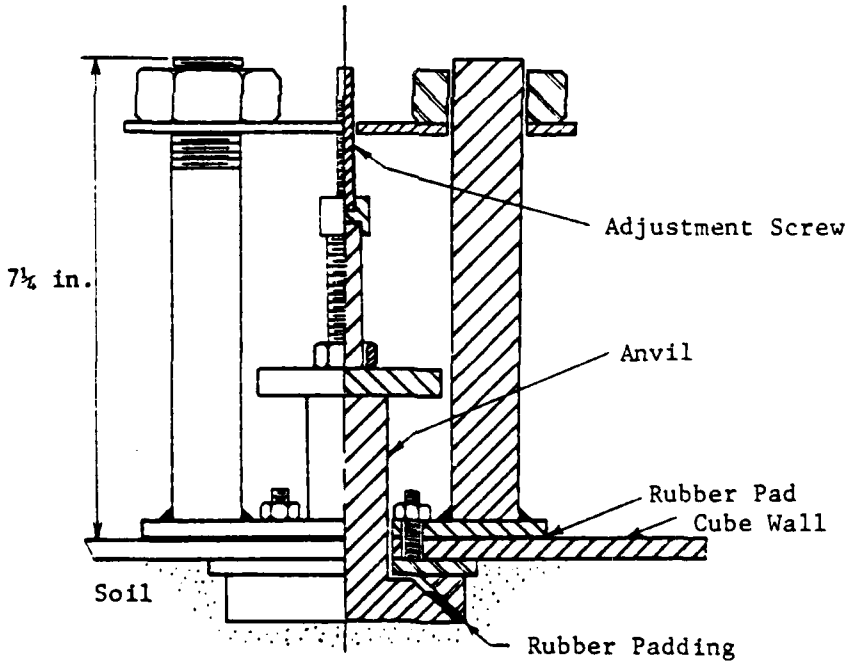

b. Section "A-A"

Fig. 9 - Excitation Hammer in Each Port of Triaxial Cube

Rubber padding is placed between the anvil and internal frame to permit movement of the anvil inside the frame.

To generate distinct waves, intimate contact between the soil and base of the anvil is essential. The base of the anvil in contact with the soil is knurled to maximize this contact.

Vibrations in the wall of the cube become background noise on the waveform records and must be minimized wherever possible. For this reason, rubber padding has been placed between the external frame and wall of the cube as shown in Fig. 9.

The excitation port assembly protrudes approximately 7 in. outside of the cube and about 0.9 in. inside of the cube. These sizes were chosen for ease of handling and use. The base of the anvil which contacts the soil is also 3 in. square and was selected after investigation of the effect of base size on wave generation.

Wave propagation tests were performed in the Dynamic Response Test Facility at the Balcones Research Center of The University of Texas. This facility is composed of sand that is very similar to that which will be used in the initial tests in the cube. Three different sizes of base plates were tested: 2-3/16 in., 3-1/4 in., and 4 in. in diameter. The test set-up mirrored the conditions in the cube. Horizontal and vertical geophones were buried at depths of 12 in. and 24 in. below the ground surface for monitoring the waveforms in a similar fashion to the accelerometers in the cube. The base plates were placed on the ground surface (representing the soil boundary in the cube) directly over the buried geophones. The base plates were then struck vertically and horizontally to generate P-waves and S-waves in the soil. Polaroid pictures of the traces on an analog oscilloscope were used to record the waveforms monitored by the geophones. Typical records are shown in Fig. 10. From records such as these, it was concluded that the distinctness of the P-wave arrival was the same for all bases, but there was a slight improvement in the distinctness of the S-wave arrival with increasing base size. Since a small port is desirous in the cube to simulate a point source and since the improvement in the S-wave was greater between the 2-3/16 in. and 3¼ in. dia. plates than between the 3¼ in. and 4 in. dia. plates, a 3-in. square base plate for the anvil

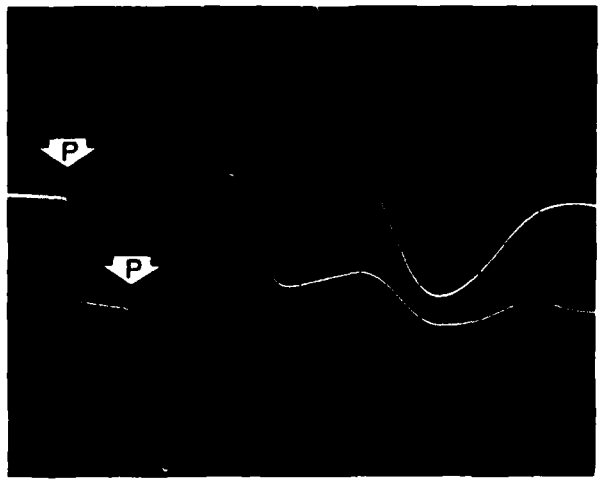

0.001 sec $\qquad v_p = \frac{1 \text{ ft}}{0.001 \text{ sec}} = 1000 \text{ fps}$

a. Travel Time Record of Compression Wave Using Vertical Geophones

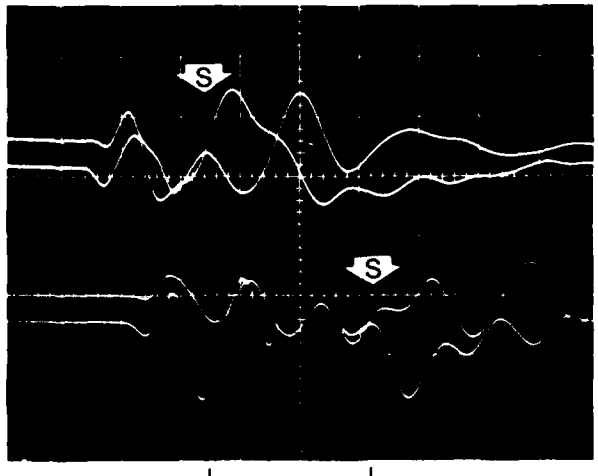

0.0028 sec

$v_p = \frac{1 \text{ ft}}{0.0028 \text{ sec}} = 360 \text{ fps}$

b. Travel Time Record of Shear Wave Using Horizontal Geophones

Fig. 10 - Typical Travel Time Records for Surface Source and Embedded Receivers

was chosen which has about the same contact area as the 3½ in. dia. circular plate.

2.4 Monitoring and Recording Systems

Compression and shear waves propagating through the sand in the cube are monitored and recorded with the electronics shown schematically in Fig. 11. The core of this measurement system is a spacial array of three-dimensional (3-D) accelerometers buried in the soil. Three, 3-D accelerometers are placed along each of the three principal axes of the sand mass as shown in Figs. 4 and 5. A spacing of about 1.5 ft is used between adjacent 3-D accelerometers. Spacing between the accelerometers closest to the cube wall and the wall is about 2 ft so that minimum intereference is caused by reflections of the waves off of the walls.

Each 3-D accelerometer package is composed of three accelerometers rigidly attached in a 1.75 in. square wooden block as shown in Fig. 12. One accelerometer is aligned along each of the three principle axes of the cube. The wooden block was chosen as the 3-D accelerometer housing to replace exactly the weight of the sand displaced by the 3-D package and to minimize the stiffness difference between the block and surrounding sand.

Monitoring of low-amplitude wave propagation through the sand requires highly sensitive accelerometers. The accelerometers used have a sensitivity of 0.001g and a cross sensitivity (sensitivity to movement not along the major axis) of less than 1 percent. They are small in size and weight so as to create minimum interference as a wave passes and to track closely the particle motion of the wave.

The electrical cables from the accelerometers pass through two ports in one side of the cube. The 21 wires are connected to a switching box outside the cube so that any three accelerometers can be connected with charge amplifiers and then recorded on the digital oscilloscopes.

A normal test requires that three accelerometers be monitored simultaneously. The three accelerometers of interest lie along the axis

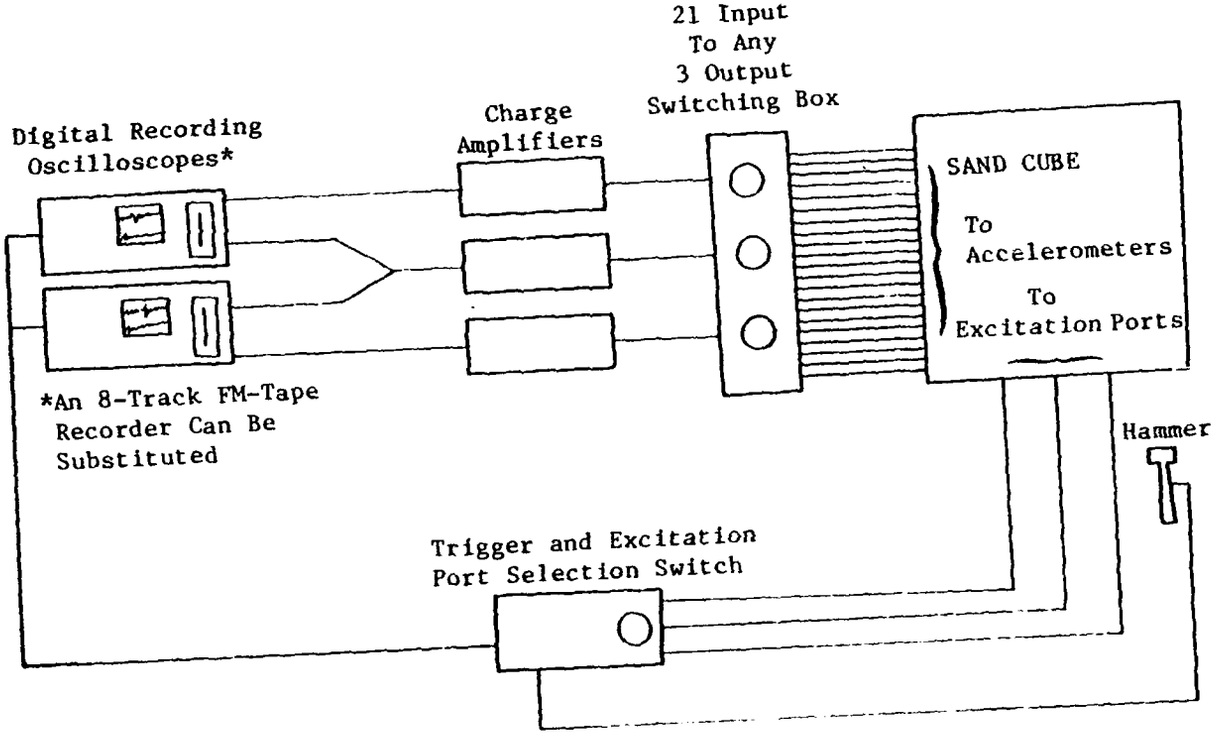

Fig. 11 - Schematic of Monitoring and Recording Systems

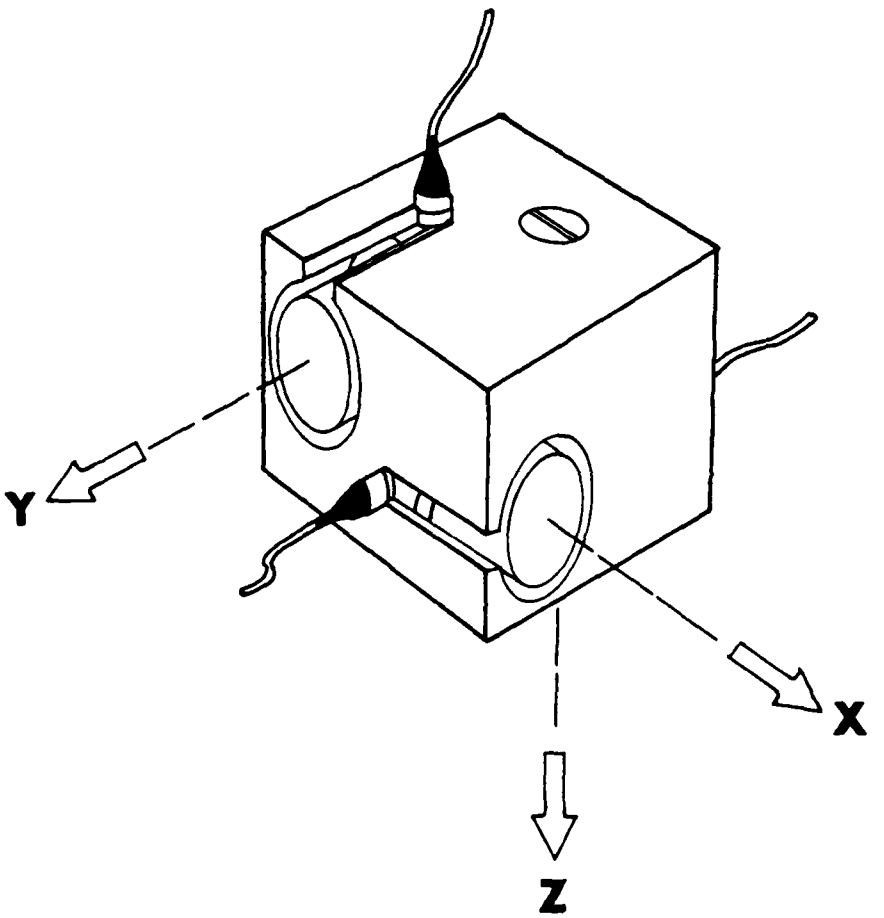

Fig. 12 - Isometric View of 3-D Accelerometer Package

of the port being excited and are sensitive along the same direction as the motion of the anvil. Because each digital oscilloscope is only a two channel device, two oscilloscopes are required to record the output from the three accelerometers with one accelerometer output being duplicated between the two oscilloscopes for reference. The oscilloscopes are triggered electronically when the hand held hammer strikes the anvil of the excitation port. At this instant, a voltage drop is sent from the trigger box to the oscilloscope by means of a resistance-capacitance circuit which initiates the recording cycle. The trigger has a switch to select any of the three excitation ports in use.

With the digital oscilloscope, each waveform is recorded on a floppy diskette for later recall and study. Saving a waveform digitally also permits direct reading of arrival times and particle motions, plus the possibility of direct computer hook-up. In the future, rather than the oscilloscopes, an FM digital tape recorder or spectrum analyzer can be used permitting recording for analysis in the laboratory at a later date or direct fourier series analysis.

2.5 Sand Placement

The object of the sand placement system is to fill the cube with sand of a uniform density over the entire height of the cube. The method of raining sand through air was chosen over other methods because of the efficiency and uniformity of placement attainable with this method. Raining sand through air has been shown to yield uniform, medium-dense samples when the height of fall is 2.5 ft or greater (Kolbuszewski, 1948; Beiganousky and Marcusson, 1976). Marcusson and Beiganousky (1977) also found that when they rained sand through several layers of screens with openings of 0.25 in., the variation in density was only $\pm$ 0.5 pcf for a given drop height.

The raining system is shown in Fig. 13. It is composed of a "V" shaped hopper which can be moved across the top of the cube. The hopper has a gate for flow control and two screens with openings of 0.25 in. all spaced approximately 3 in. apart at the bottom of the hopper. The hopper sits on a 30-in. high wooden collar which bolts to the top of

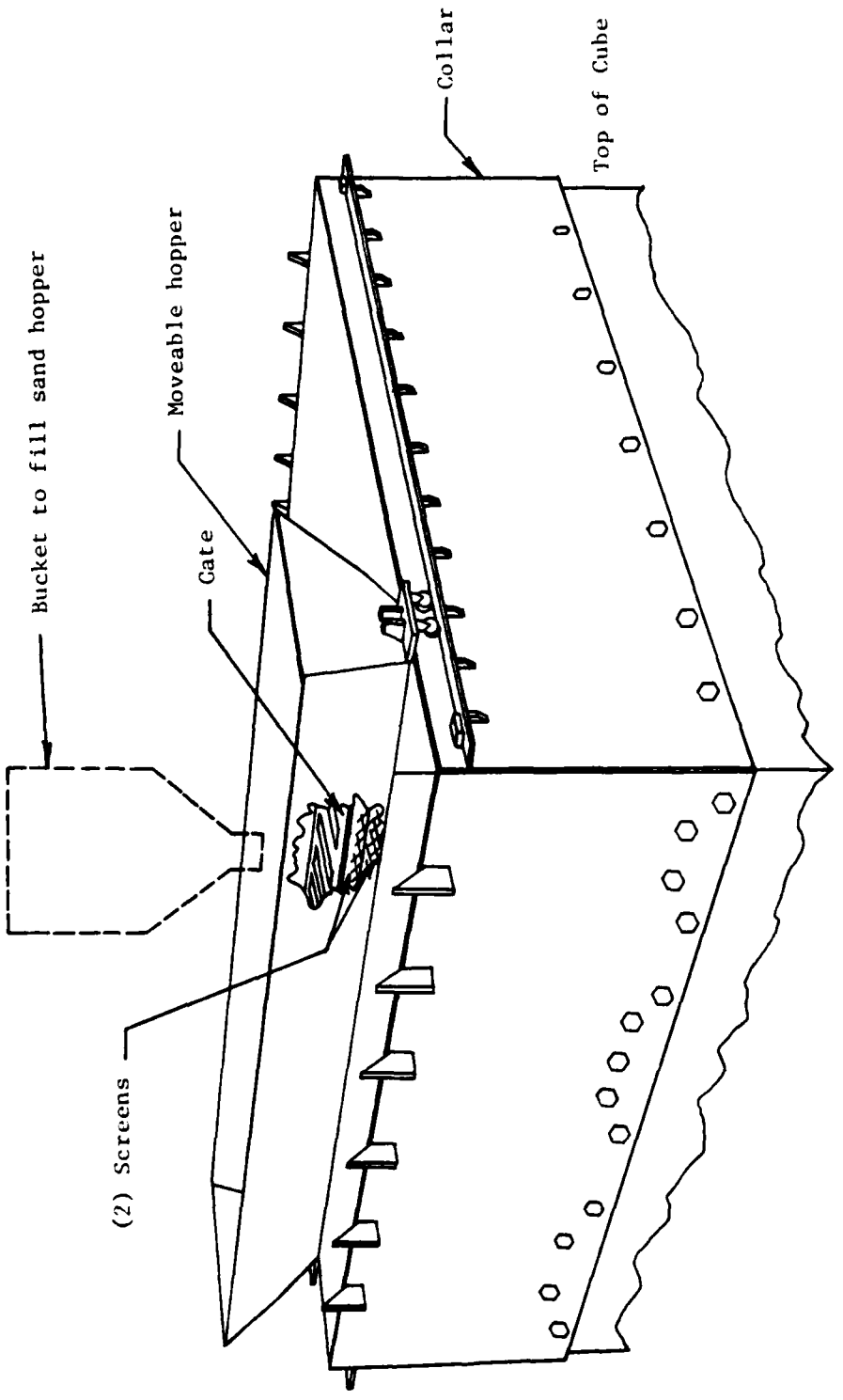

Fig. 13 - Sand Placement System

the cube so that the drop height of the sand in the cube ranges from 2.5 ft to 9.5 ft. For convenience, the bolt holes in the collar match those in the cube so that the collar can be easily attached. The entire system is disassembled and stored when not in use.

The method for placing sand is as follows. A large bucket (the same one used for placing wet concrete) is filled with sand and lifted by the crane over the moveable hopper. The hopper is filled with sand from this bucket. When the hopper is full, the hopper gate is opened, and the hopper is moved at a constant rate along the rails of the collar attached to the top of the cube. A curtain of sand drops and forms a uniform layer in the cube, at the same time compacting the layers below it. The outlet at the bottom of the hopper is 8-in. wide and 7-ft long, the same length as the cube. The volume held by the rainer is approximately 7 cu ft which results in depositing a layer slightly more than 1 in. thick for each filling. When the hopper is empty, the gate is closed and the process repeated.

Raining is stopped at those times when the accelerometers are to be placed at their required locations.

3.0 SAND USED IN INITIAL TESTING

The sand to be used in the initial stage of wave propagation testing has been selected and delivered to the Ferguson Structural Research Laboratory at the Balcones Research Center. The sand is a medium to fine washed mortar sand which classified as SP in the Unified Soil Classification System. The results of grain size analyses performed on four sand samples are shown in Fig. 14. The average grain size curve shows the uniform grading of this mortar sand which makes the sand well suited for the planned testing. Because of the uniformity in size of the sand grains, the sand can be rained into the triaxial cube without significant segregation.

In the initial testing, the sand will be tested in a dry state.

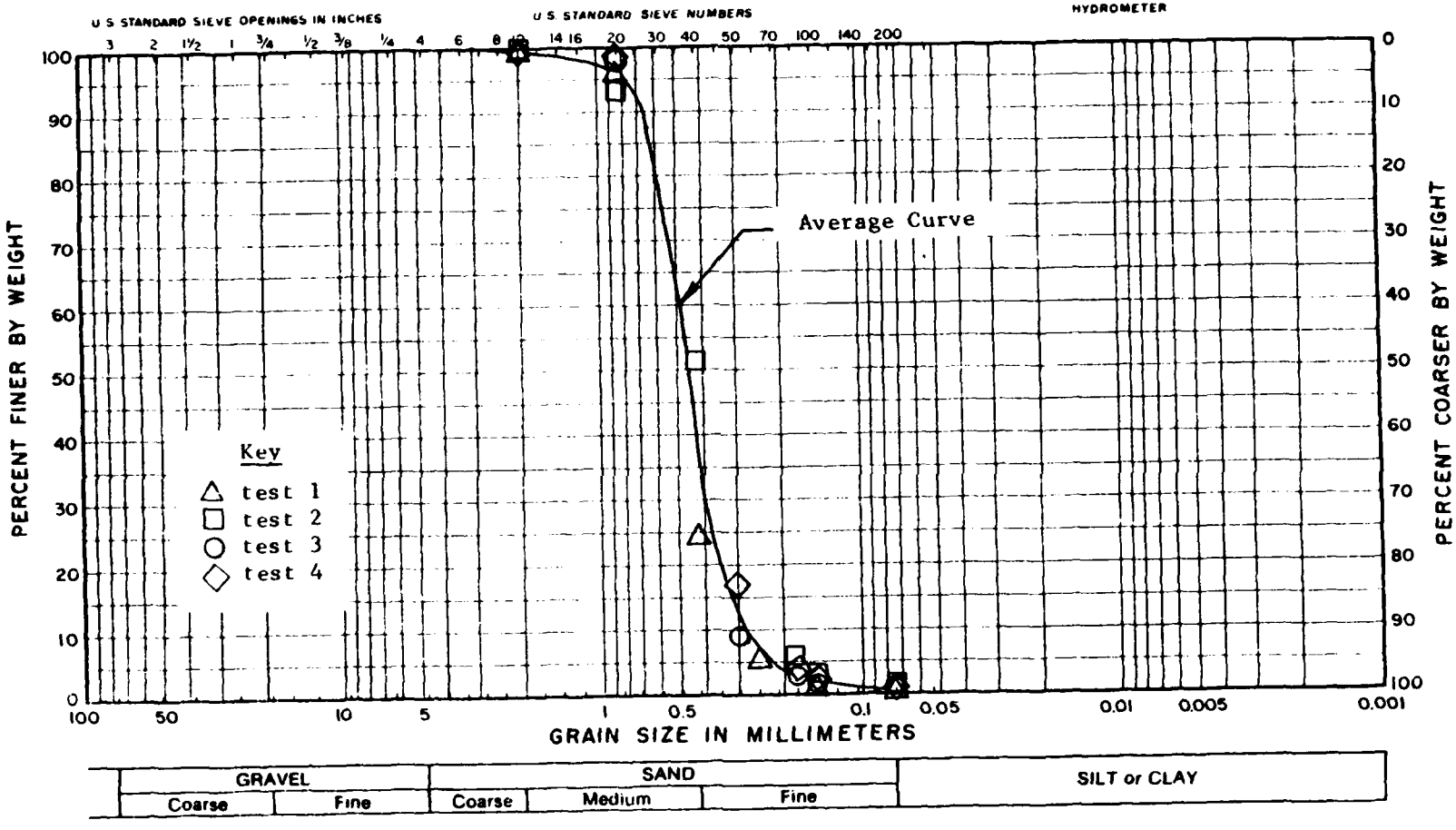

Fig. 14 - Grain Size Analysis of Washed Mortar Sand

3.1 Dynamic Testing

Dynamic soil property tests have also been performed on the sand. Resonant column equipment was used to evaluate the shear modulus, G, and material damping ratio, D, of the sand over a range in hydrostatic confining pressures from 2.5 to 80 psi. Both low-amplitude and intermediate-amplitude tests were used to evaluate G and D. Low-amplitude tests are defined as those tests in which the single-amplitude shearing strain, γ, did not exceed 0.001 percent. Intermediate-amplitude tests are those tests in which shearing strains were in the range of 0.001 to about 0.01 percent.

The significance of low-amplitude testing is that dynamic soil properties are essentially constant in this strain range (Hardin and Drnevich, 1972a,b) and it is the strain range expected in the initial tests in the triaxial cube. At shearing strains above 0.001 percent, dynamic soil properties may be influenced by strain amplitude depending on the soil type, strain amplitude, and confining pressure.

3.2 Low-Amplitude Dynamic Properties

Two series of low-amplitude tests were performed to determine the effect of the effective mean principal stress, $\bar{\sigma}_o$, on G and D. Different initial void ratios of 0.59 and 0.76 were achieved in each test series. In addition, the second test series included an unloading pressure sequence to study the effect of stress history on the dynamic properties.

The variation in the low-amplitude G with effective hydrostatic confining pressure is shown in Fig. 15. There is a linear relationship on a log-log plot with the shear modulus increasing as confining pressure increases. Shear modulus decreases as void ratio increases for any confining pressure. However, the decrease in shear modulus with increasing void ratio does not significantly change the slope of the log G - log $\bar{\sigma}_o$ relationship.

Based on the low-amplitude results shown in Fig. 15, the shear modulus can be expressed as (after Hardin, 1978)

$$G_{max} = \frac{C}{0.3 + 0.7e^2} P_a^{1-n} \bar{\sigma}_o^{n} \qquad (1)$$

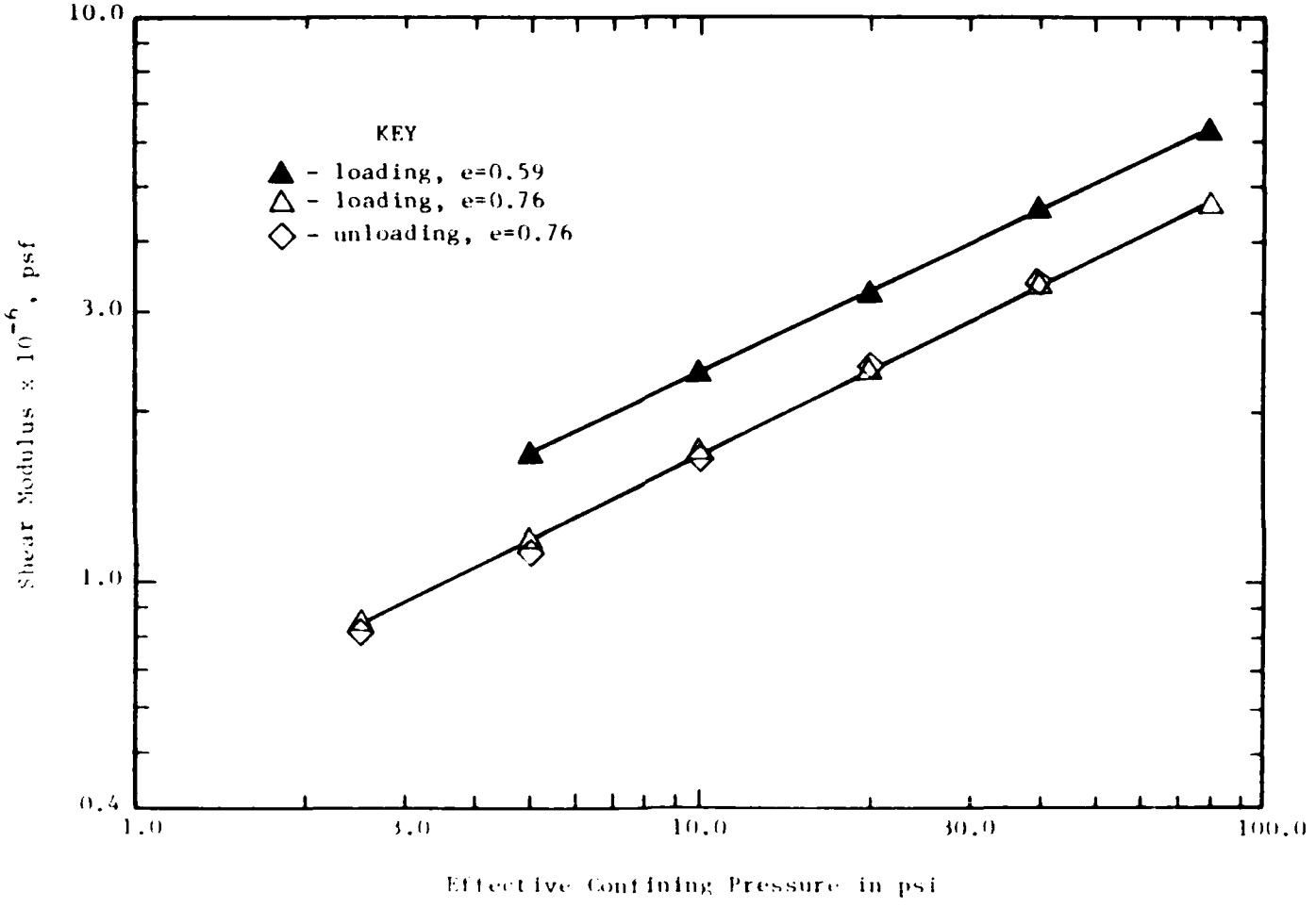

Fig. 15 - Variation in Low-Amplitude Shear Modulus with Confining Pressure

where: G_{max} = shear modulus in psi,
C = constant (dimensionless),
$\bar{\sigma}_o$ = effective confining pressure in psi,
P_a = atmospheric pressure in psi,
e = void ratio, and
n = slope of log G - log $\bar{\sigma}_o$ relationship.

Average values for C and n were determined and found to be 700 and 0.49, respectively. These values of C and n result in calculated shear moduli within $\pm$ 7 percent of the measured shear moduli for the sand. Therefore, Eq. 1 can be used to predict the shear modulus (and shear wave velocity) of the sand in the triaxial cube when the loading is hydrostatic.

The unloading pressure sequence shown in Fig. 15 for this sand indicates that previous stress history has little effect on the shear modulus and for all practical purposes can be neglected.

The variation in low-amplitude material damping with confining pressure is shown in Fig. 16 for the sand tested at both void ratios. The results show that D decreases as confining pressure increases, with the rate of decrease becoming less significant as confining pressure increases. For these test data, there does not appear to be a significant effect of void ratio upon the damping in the sand for any confining pressure. However, careful attention may have to be paid to stress history.

3.3 Intermediate-Amplitude Dynamic Properties

One intermediate-amplitude test series was performed to determine the effect of shearing strain amplitude on the shear modulus and material damping of the sand in this strain range. This test series was performed at the same set of confining pressures as the low-amplitude tests and with an initial void ratio of 0.76.

The variation in shear modulus with shearing strain amplitude at each confining pressure is shown in Fig. 17. As seen in the figure, shear modulus decreases slightly with increasing shear strains for confining pressures less than about 40 psi. For confining pressures of 40 psi or above, shear modulus is essentially constant over the magnitude of shearing strains tested. However, for testing purposes in the triaxial

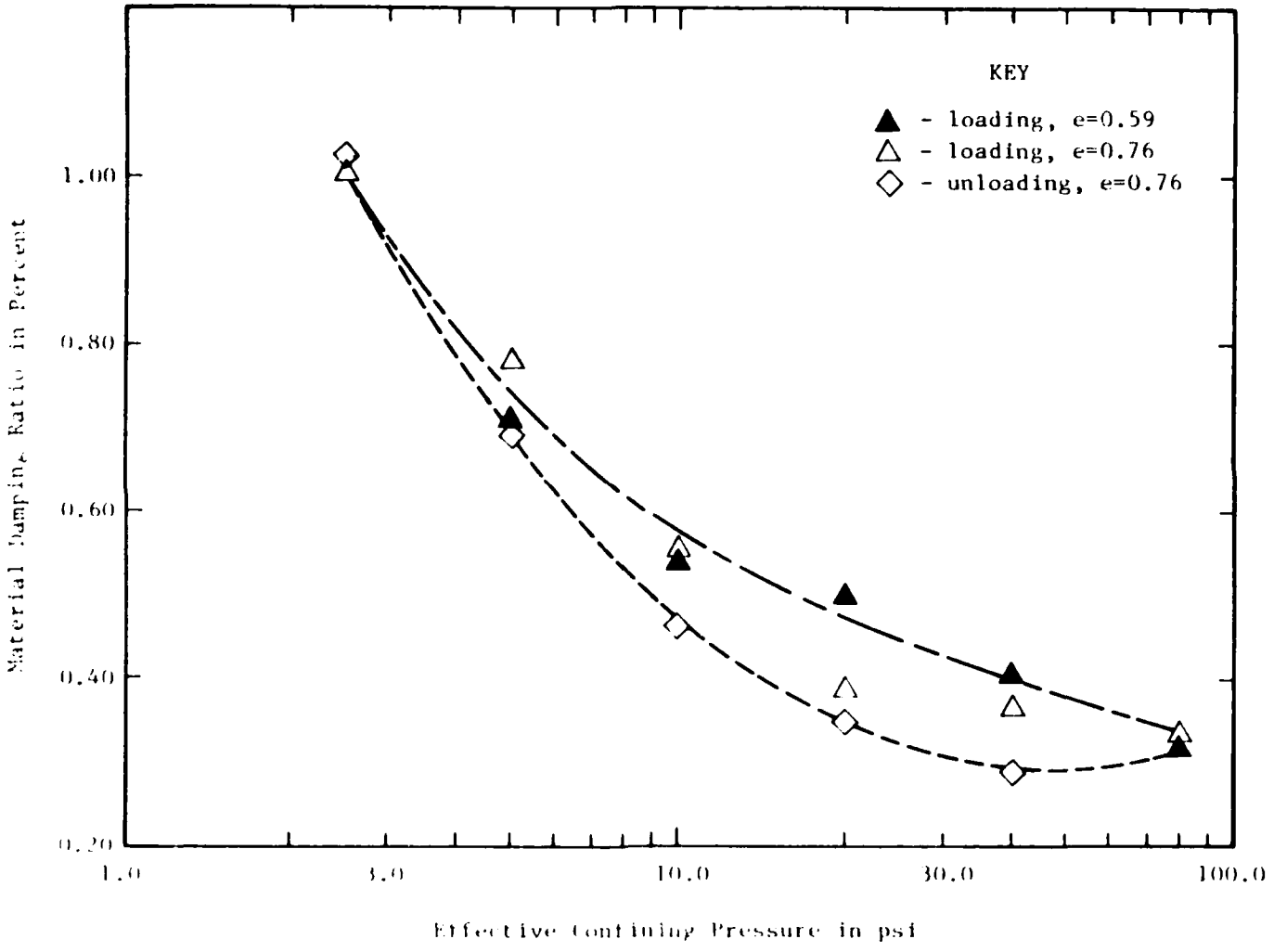

Fig. 16 - Variation in Low-Amplitude Damping Ratio with Confining Pressure

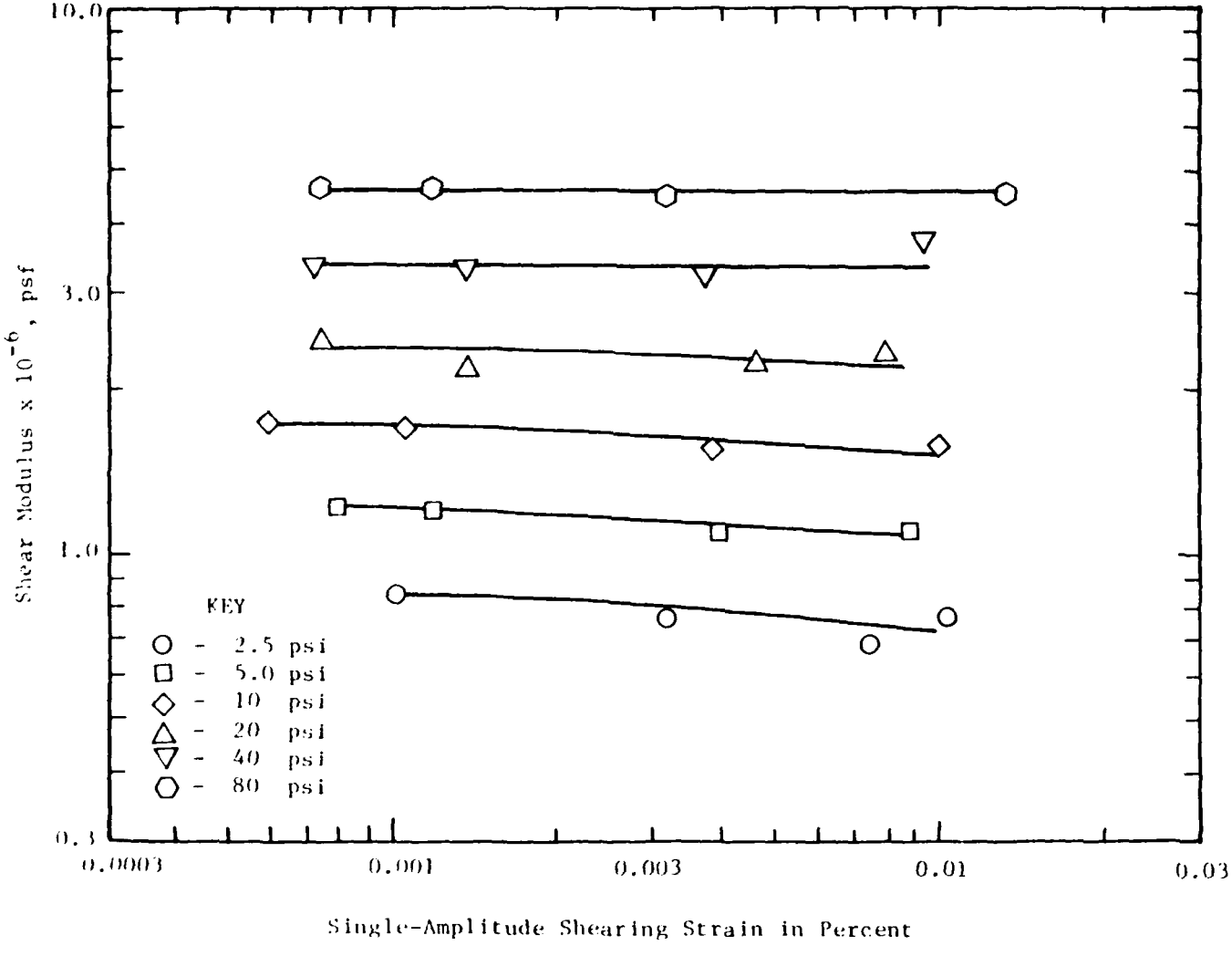

Fig. 17 - Variation in Shear Modulus with Shearing Strain

cube, shear modulus can be considered constant unless γ exceeds 0.003 percent. As a result, shear wave velocity can also be considered constant up to this strain amplitude.

The variation in material damping ratio with shearing strain amplitude is shown in Fig. 18 at each of the confining pressures tested. The figure shows that damping ratio increases with increasing strain amplitude and for shearing strains above about 0.001 percent. This variation is largest at the lowest confining pressure. These results show that for any testing in the cube above a strain of 0.001 percent, care must be taken in analyzing the data to account properly for any strain amplitude effect.

4.0 ANALYTICAL STUDIES

While most of the effort during the first year of the project has been devoted to the design and construction of the triaxial cube, some work has also been performed implementing computer capabilities which could be used in the future for interpretation of the experimental data.

The first problem at hand was determination of the effect of the much stiffer (almost rigid) 3-D accelerometers embedded in the sand on the characteristics of P- and S-waves propagating through the soil (scattering or filtering effect). Most of the effort in this work concentrated on S-wave measurements because of the greater difficulty involved in these measurements. Two approaches were contemplated for the solution of this problem: a formulation based on the use of the boundary integral equation (or boundary element) method and a more classical discretization using finite elements.

The boundary integral equation method is particularly appropriate to study the filtering effect of one or more rigid inclusions on waves propagating through a full elastic space, since then only the boundaries of the inclusions must be discretized. For the particular case at hand with three rigid inclusions along any principal axis (and considering only one principal axis), the formulation of the problem in the frequency domain requires the solution of a system of 54 equations with 54 unknowns for each frequency. The solution for a transient excitation can then be obtained using Fourier transforms.

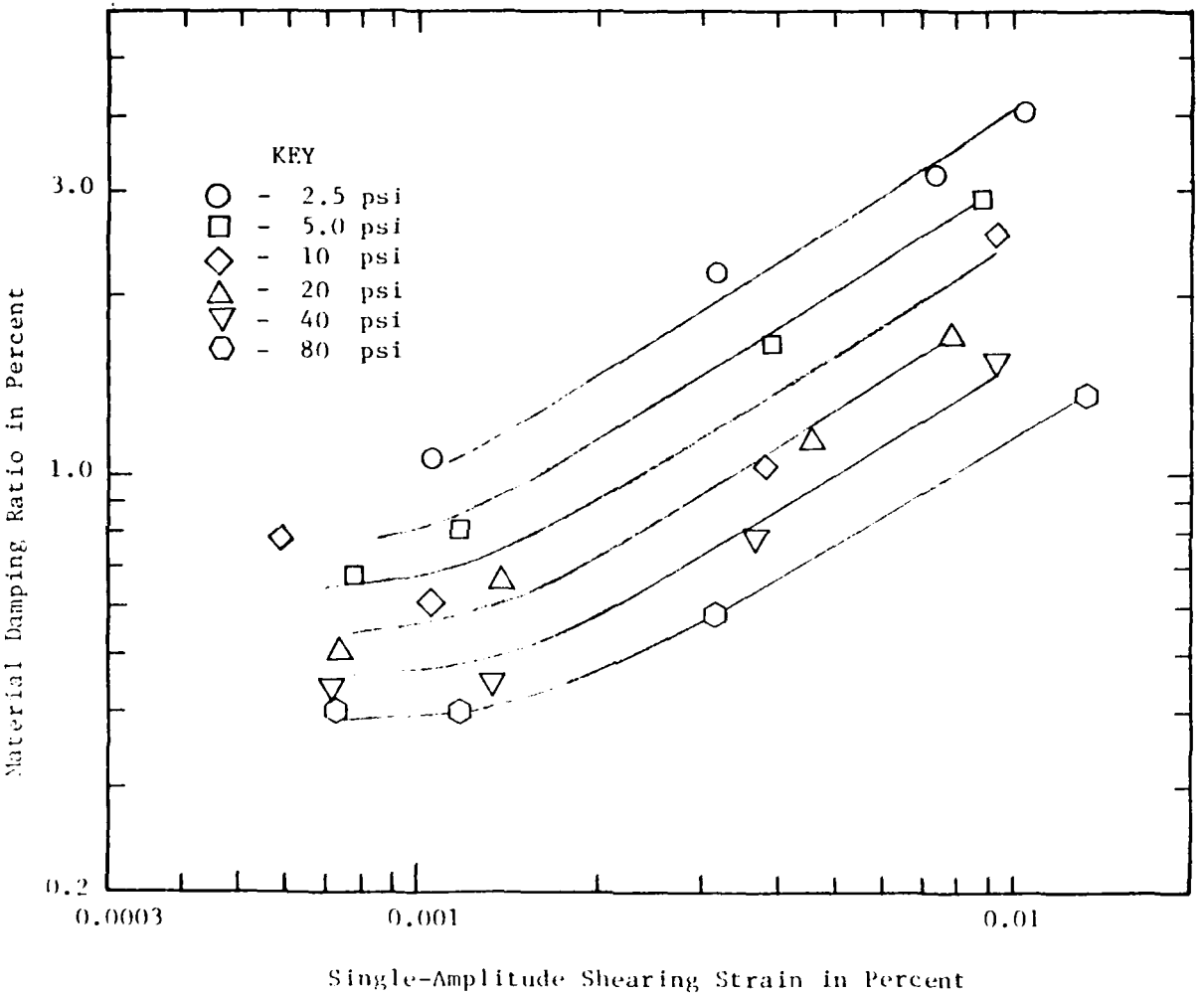

Fig. 18 - Variation in Material Damping Ratio with Shearing Strain

For the actual case of the cube, by opposition to a full space, it would also be necessary to discretize its outer surface. A discretization appropriate for wavelengths of the order of 1 ft would lead to a system of 56,502 equations with 56,502 unknowns for each frequency. By taking advantage of symmetry and antisymmetry conditions, the number of degrees of freedom can be reduced to 23,574, but the two matrices associated with tractions and displacements are fuliy populated, which makes the solution prohibitively expensive.

If three-dimensional brick elements (with linear displacement expansion) are used, an appropriate discretization of the cube into finite elements for wavelengths of the order of 1 ft or larger requires a mesh size of 1.5 in. or 56 elements per side (1.5 in. is also the size of the rigid inclusions). This leads to a total of 175,616 elements or 185,193 joints with three degrees of freedom per joint and a bandwidth of 9582. Solution of this problem would again be impractical by any method which requires assembling the total stiffness matrix or solving the coupled system of equations. It is possible, on the other hand, to solve it using an explicit integration scheme, such as the central difference formula, and marching out the solution in the time domain. While the time step of integration must be kept sufficiently small to guarantee stability and the solution is time consuming, the advantage of this approach is that it easily allows incorporation of nonhomogeneous soil properites and eventually nonlinear soil behavior.

4.1 Mathematical Model

Because of these considerations it was decided that the finite element formulation had definite advantages not only for the solution of the problem at hand but more importantly for future applications. By taking advantage of symmetry and antisymmetry, one fourtn of the cube was discretized using 28x28x55 elements with dimensions of 1.5x1.5x1.5 in. This makes the side of the cube equal to 6 ft 10.5 in. instead of the 7 ft assumed, but this small difference allows each one of the inclusions to be represented by a single rigid element. Even with these simplifications

the small memory capacity of the computer available at the University of Texas (a CYBER 175) did not allow all the degrees of freedom (141,288) to be stored in core. A computer program was implemented keeping in core at any time the degrees of freedom corresponding to two planes (2523x2=5046) and writing on disk those corresponding to one plane when the corresponding slice of finite elements has been processed, while reading in those of a new plane. Preliminary studies conducted to determine the smallest natural period and the required time step of integration indicated that some 90 to 100 steps were necessary to reproduce the arrival of the first shear waves to the central box. For this duration of response, the solution of the three-dimensional problem takes about 3 hours in the computer of the University of Texas, 50 percent of this time being associated with the transfer of data from primary to secondary memory and back.

Since only a small number of fully 3-D analyses were possible within the budget of the project, it was decided to implement also a two-dimensional (2-D), plane-strain solution which could be used for more extensive parametric studies. Two versions of this program were written: one taking again advantage of antisymmetry and considering a mesh of 55x28 elements (3248 degrees of freedom), and the other with the complete square (55x55 elements or 5272 degrees of freedom). The latter was used to verify the adequacy of the boundary conditions imposed on the former.

4.2 Results of Finite Element Studies

Figs. 19 through 28 show the results of the two-dimensional analyses. In all cases the boundaries are assumed to be fixed except for the two central nodes on the left face at which a sinusoidal acceleration is specified. The frequency of the excitation (specified accelerations) is 650 rad/sec corresponding to a wavelength of 1.03 ft. The smallest wavelength to be used in the experimental work will be of the order of 1 ft or eight times the dimension of the inclusions containing the accelerometers.

Figs. 19 and 20 show the accelerations of the two corner points of the central inclusion in the direction of the excitation for the case

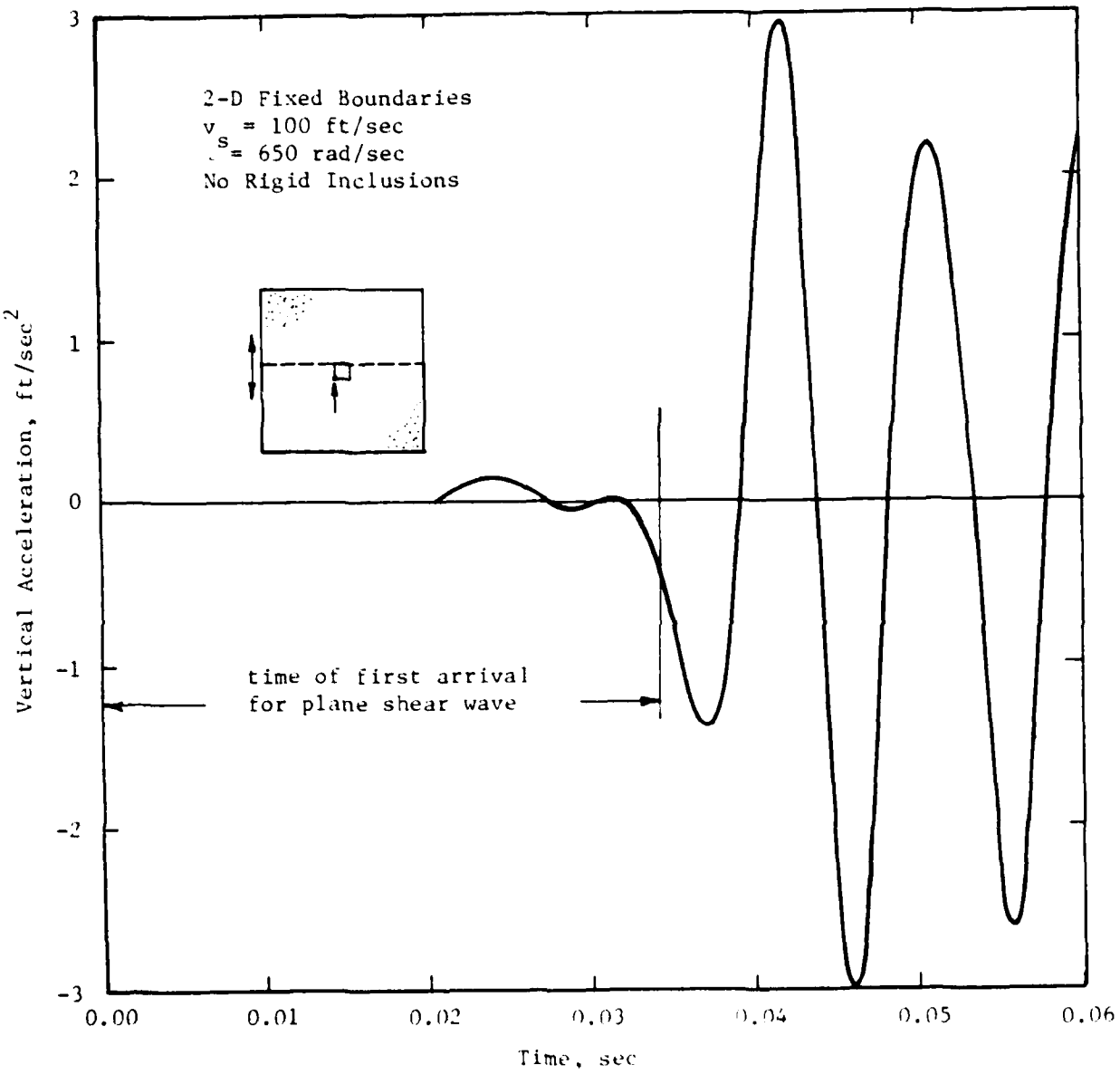

Fig. 19 - Acceleration-Time History of Left Corner of Soil Element in and Sand Mass Without Rigid Inclusions

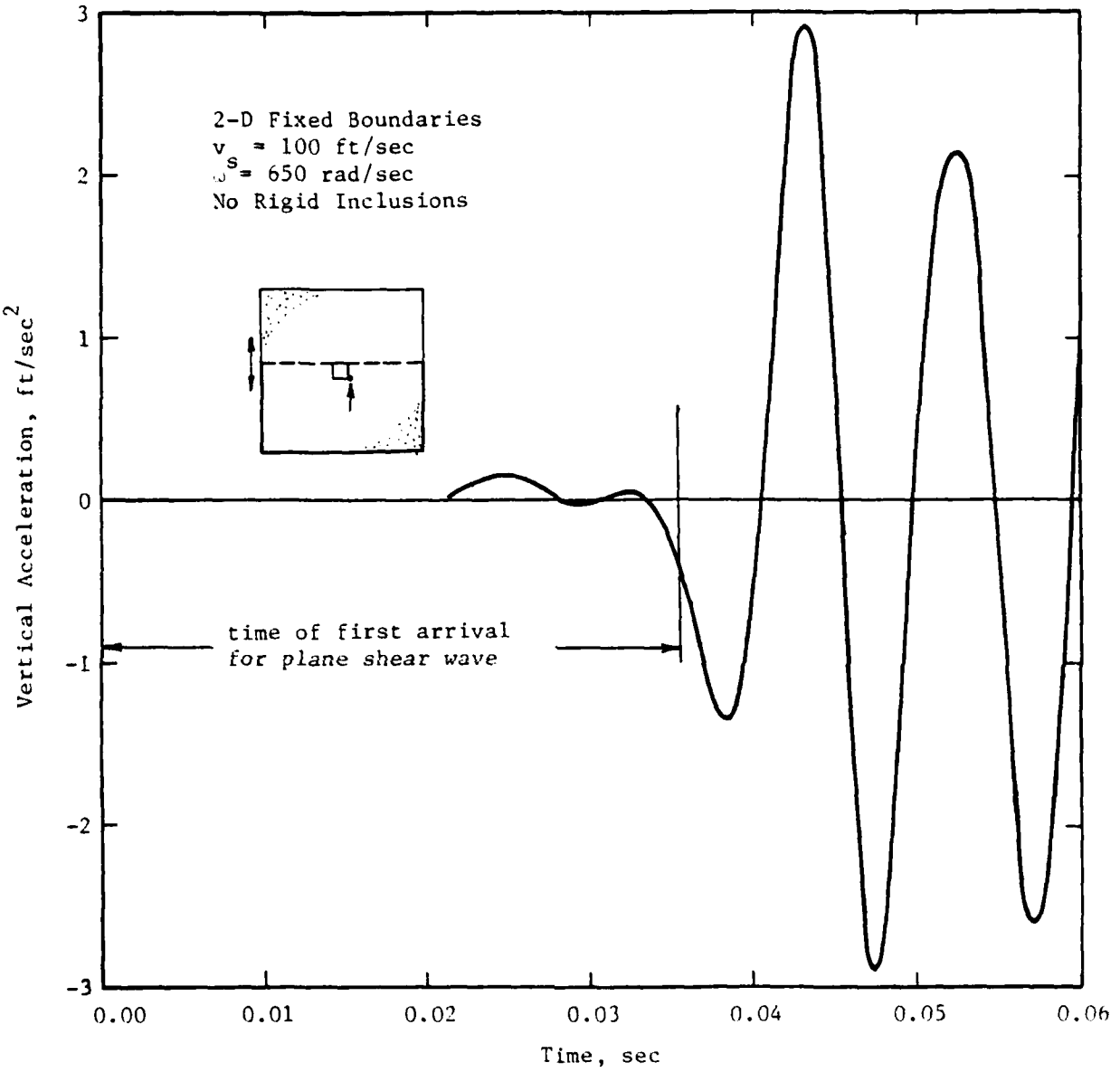

Fig. 20 - Acceleration-Time History of Right Corner of Soil Element in a Sand Mass Without Rigid Inclusions

when there is only soil (no inclusions). The time at which the shear wave would arrive at each point in the case of a plane wave front (a pure shear condition) is also indicated in the figures. The distance divided by this time would yield the shear wave velocity, v_s, of the soil. (Shear modulus equals the mass density of the soil times the shear wave velocity squared.) It is important to notice that in the case of the analysis, or in the planned experiments, there is not a condition of pure shear. Since the excitation is applied over a small area on one of the sides of the cube, both P- and S-waves will be generated. As a result some motion may be expected to occur before the theoretical arrival of the first shear wave, as indicated by the computer solution. The first shear wave can be, however, easily identified and it is interesting to observe that if its shape was rounded to make it approach more closely a half sinusoid it would pass almost exactly through the theoretical point. If, on the other hand, the shear wave velocity were estimated from the actual zero crossing point, an error of about 6 percent, which is not very significant, would be committed (the shear wave velocity would be slightly overestimated).

Figs. 21 and 22 show the corresponding results when there is only one rigid inclusion, the central one. The filtering effect of the box is evidenced by a slight decrease in amplitude of the initial oscillations but the shape of the motion is almost identical, and the same observations made above when there is no inclusion apply here. To understand better the behavior of the solution in this case, Figs. 23 and 24 show the translational and rotational accelerations of the center of the inclusion (the acceleration of any other pont of the inclusion is obtained by adding to the translational component the rotational one multiplied by the distance). Although the rotational component would seem to be larger than the translational one, it must be remembered that it has to be multiplied by a distance which is at most 1/16 ft (for the corner points or the points along the faces of the inclusion).

Figs. 25 through 28 show the results for the case when there are three rigid inclusions. A further reduction in the amplitude of the oscillations takes place, but the conclusions are basically the same as for the previous two cases.

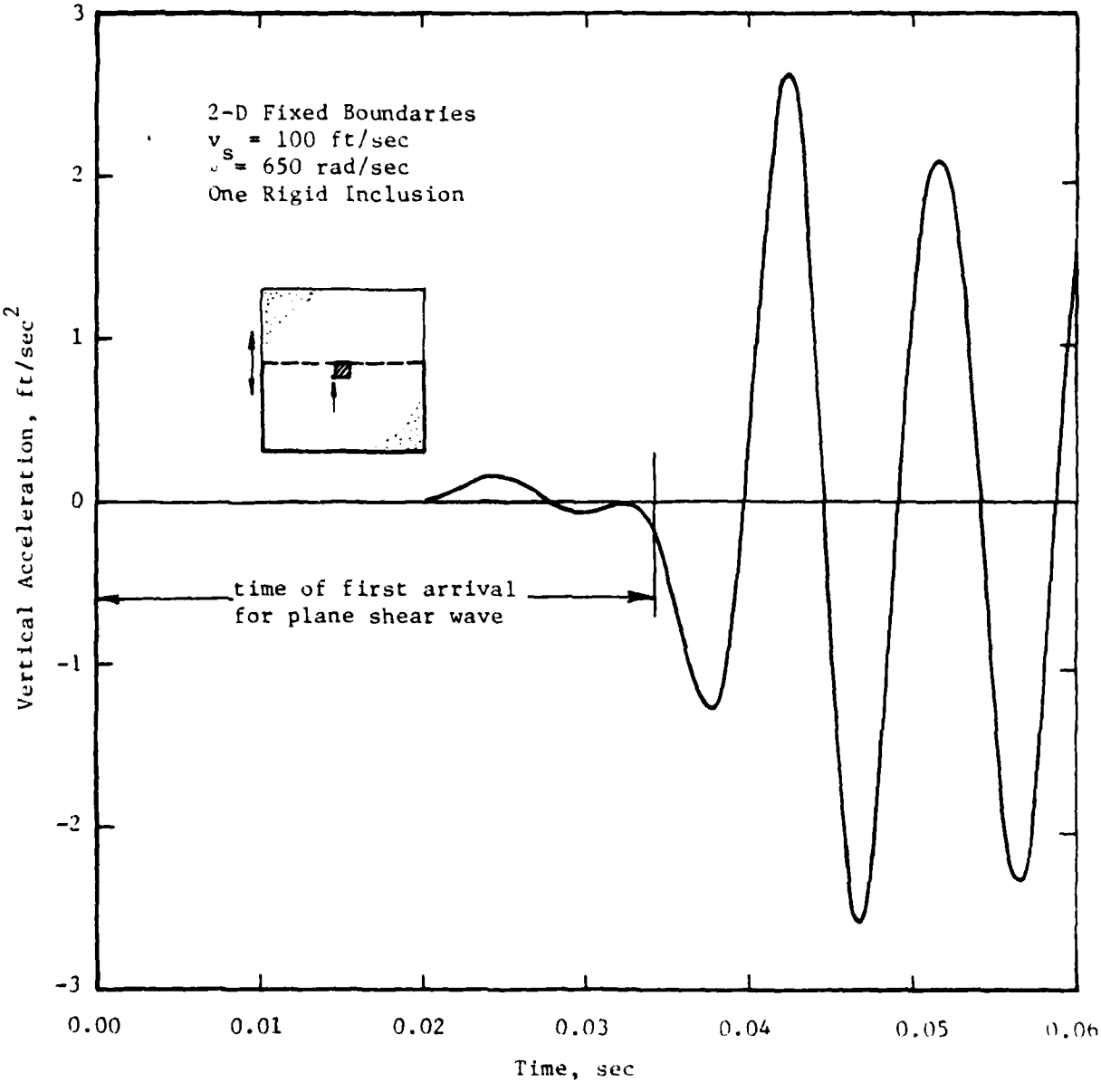

Fig. 21 - Acceleration-Time History of Left Corner of Rigid Inclusion in a Sand Mass

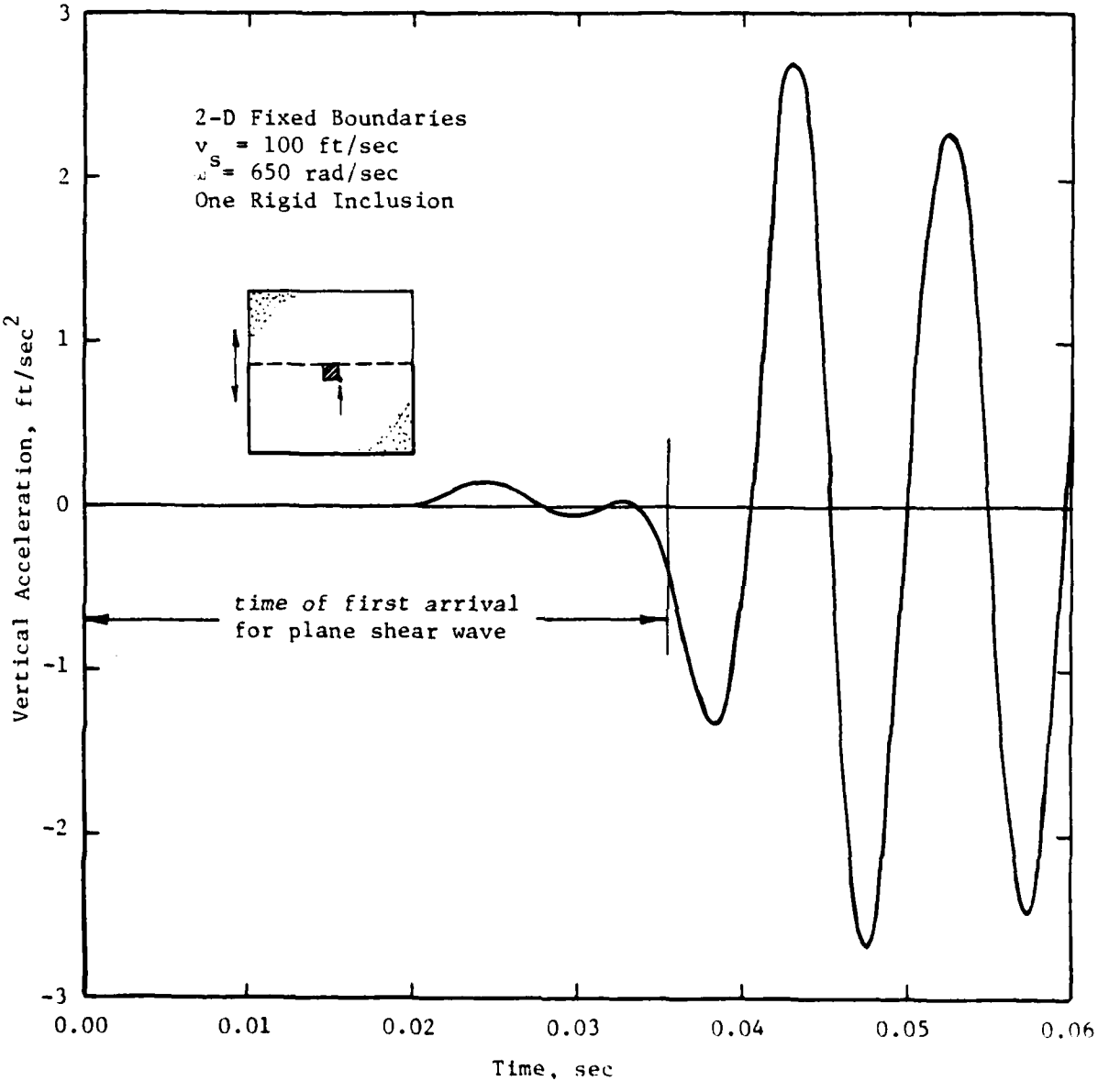

Fig. 22 - Acceleration-Time History of Right Corner of Rigid Inclusion in a Sand Mass

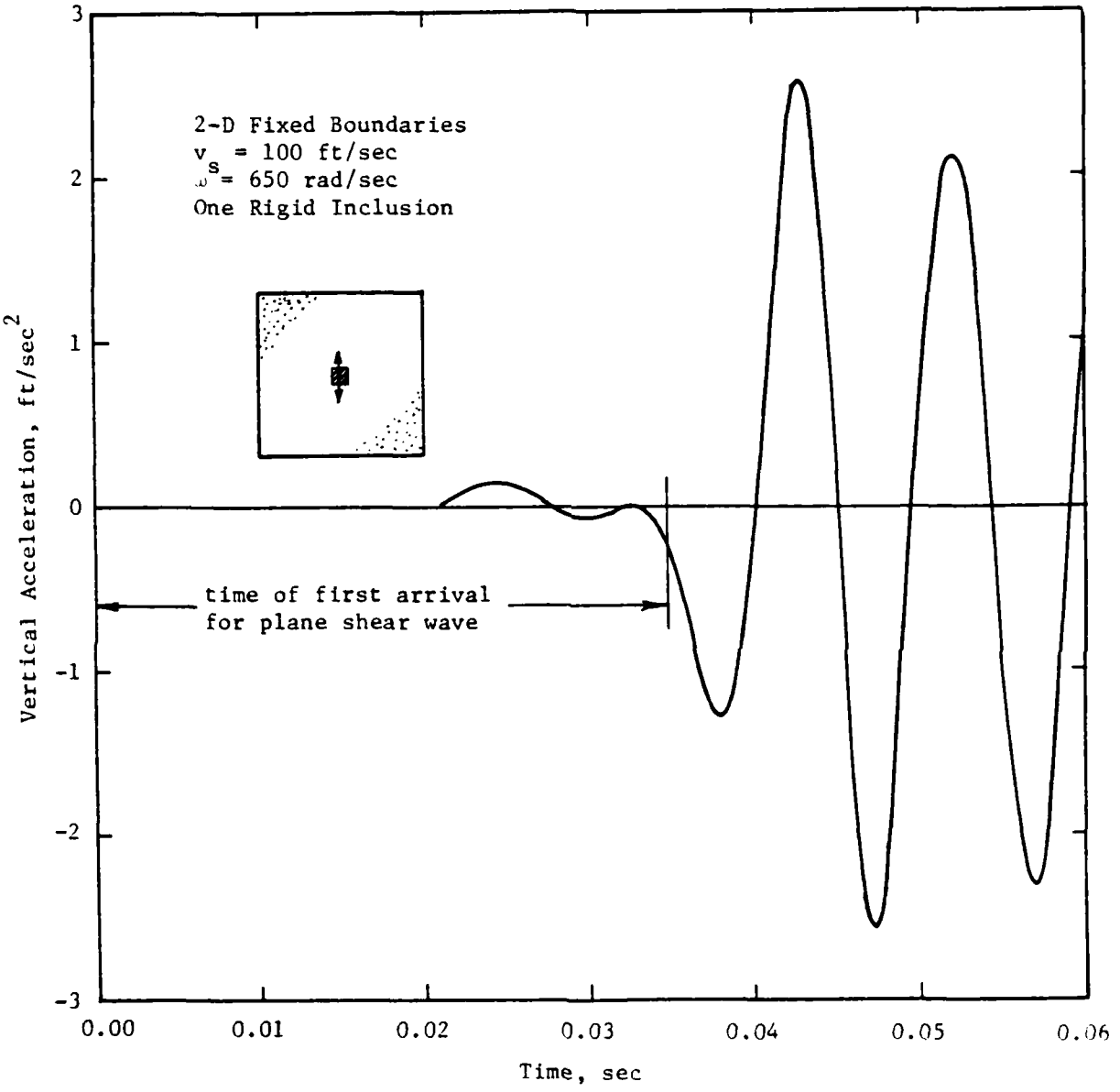

Fig. 23 - Acceleration-Time History of Center of Rigid Inclusion in a Sand Mass

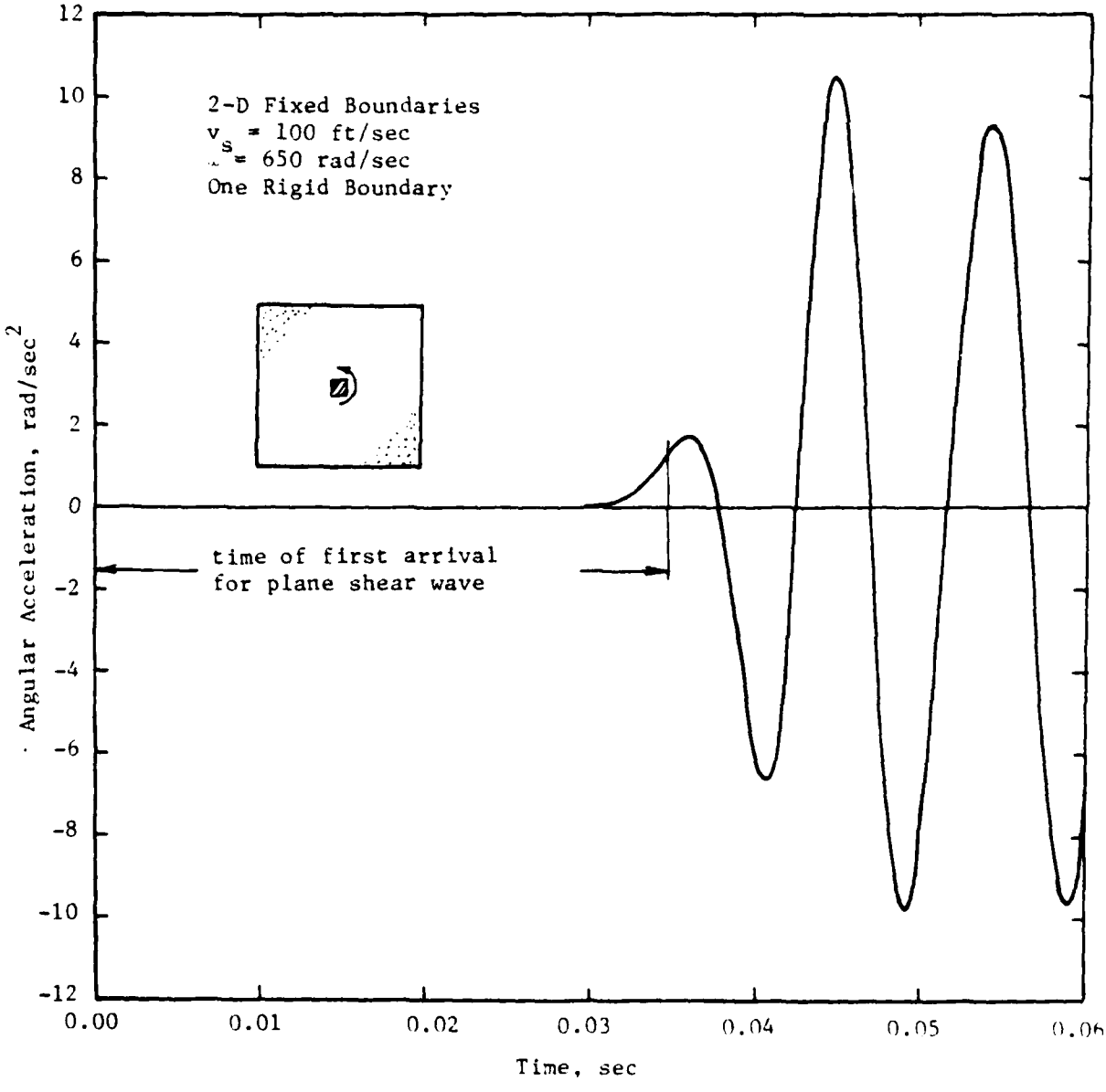

Fig. 24 - Angular Acceleration-Time History of Center of Rigid Inclusion in a Sand Mass

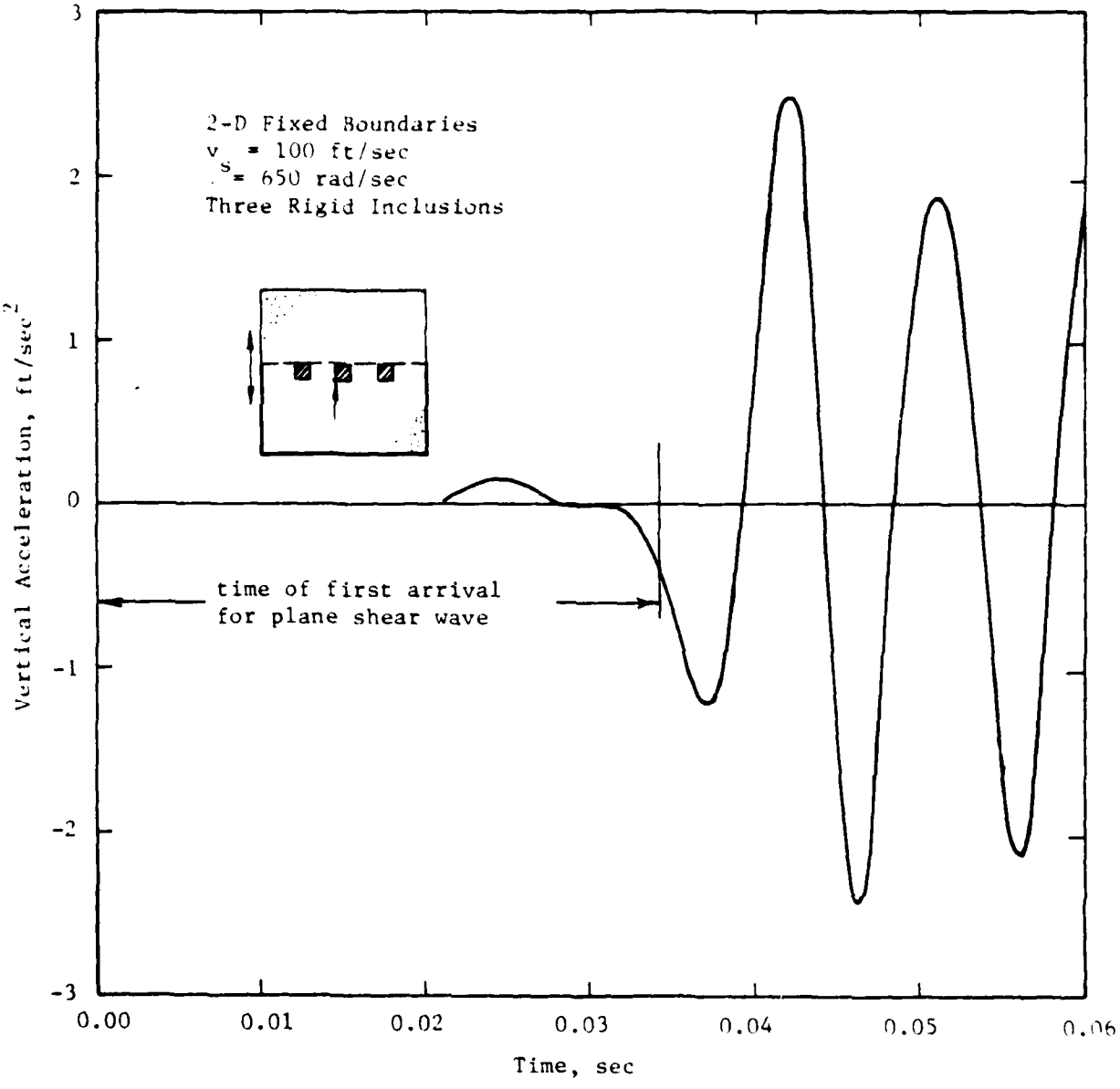

Fig. 25 - Acceleration-Time History of Left Corner of Central Inclusion in a Sand Mass with Three Rigid Inclusions

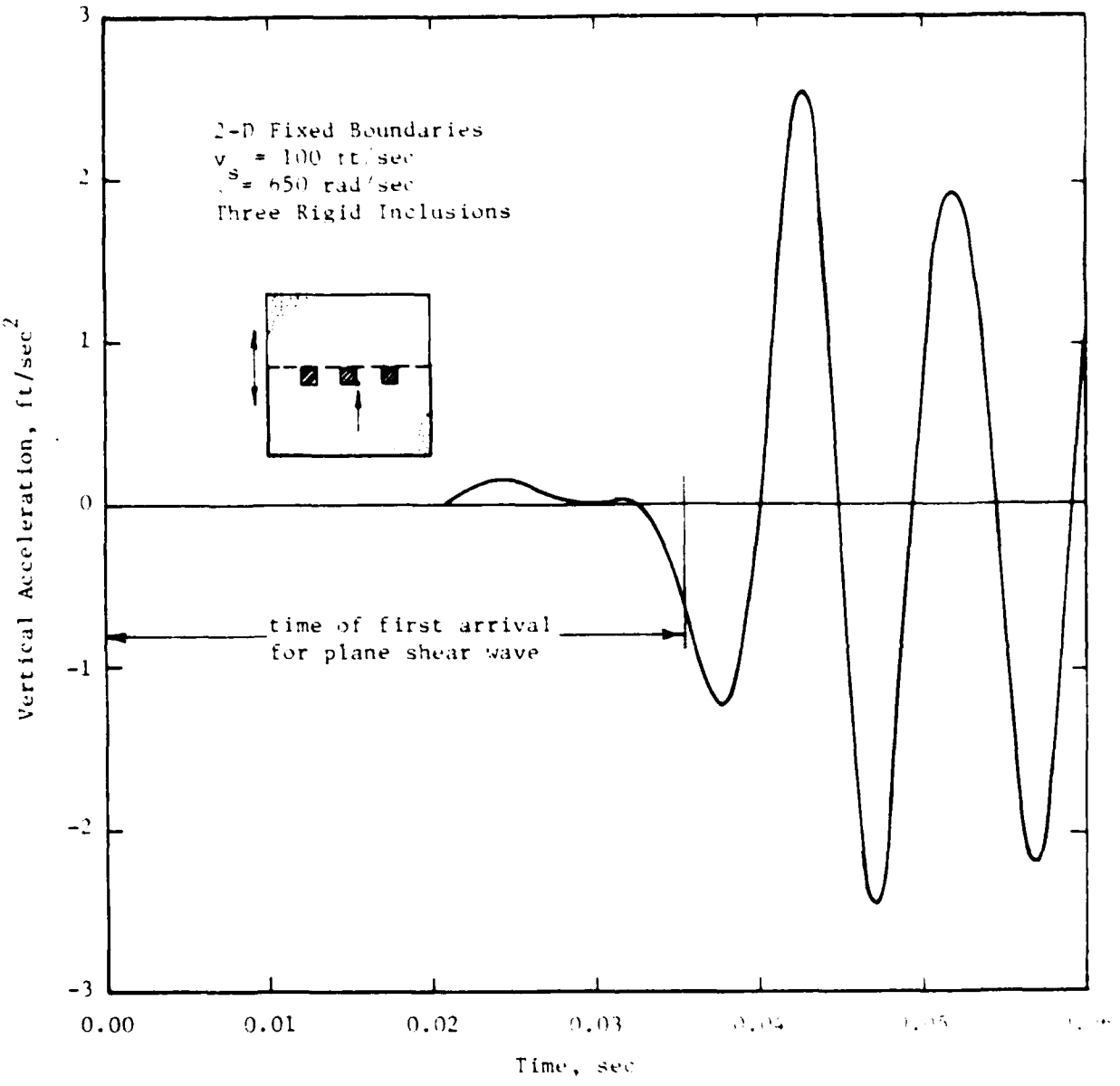

Fig. 26 - Acceleration-Time History at Right Corner of Central Inclusion in a Sand Mass with Three Rigid Inclusions

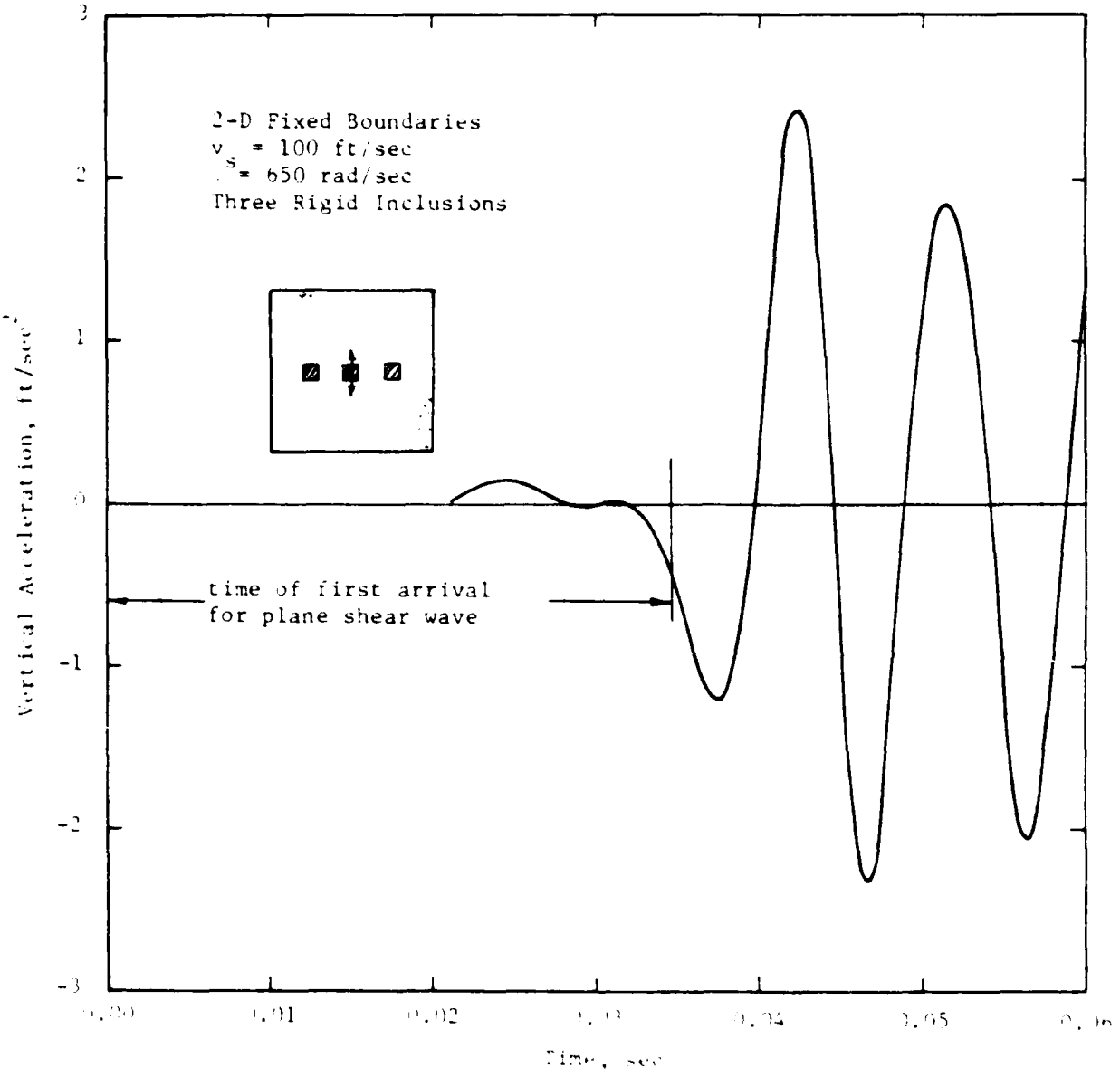

Fig. 27 - Acceleration-Time History at the Center of Central Inclusion in a Sand Mass with Three Rigid Inclusions

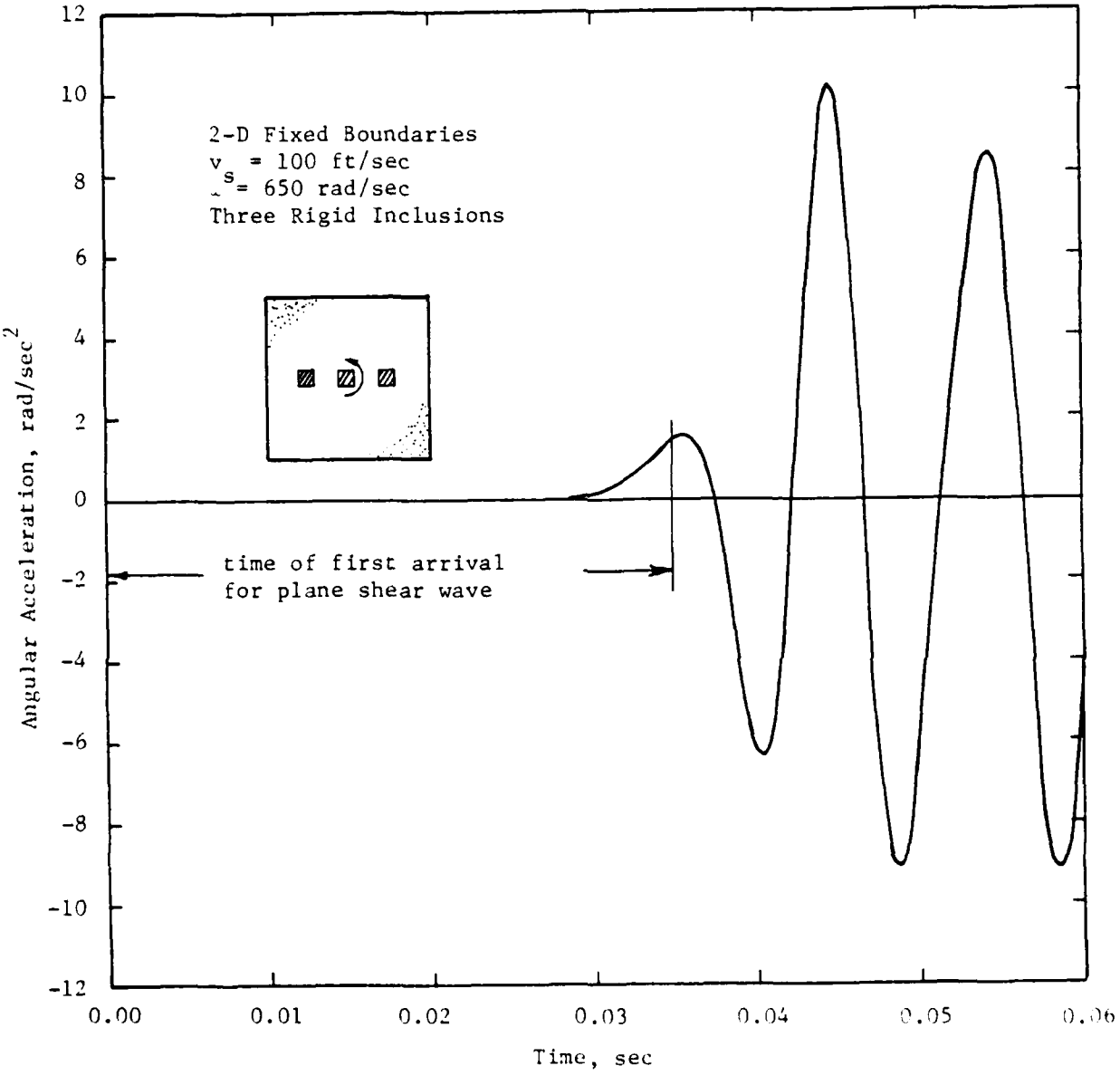

Fig. 28 - Angular Acceleration-Time History of Center of Central Inclusion in a Sand Mass with Three Rigid Inclusions

Figs. 29 and 30 show results for the 3-D case with no inclusions. In this case and in order to reduce the cost of computation, only 90 integration steps were used. It should be noticed that the general form of the solution and the observations with respect to the initial motion and the arrival of the first shear wave are the same as for the 2-D case.

4.3 Conclusions

The parametric studies conducted to date, mostly on a two-dimensional model, indicate that while there is a small filtering effect due to the presence of the idealized rigid boxes containing the accelerometers, none of the basic characteristics of the waves of importance for the experimental studies (time of arrival of the first shear wave and its shape) will be significantly affected for the range of wavelengths of interest (1 ft or larger). On the other hand, due to the fact that both P- and S-waves are generated, estimation of the time of arrival of the first shear wave may involve a small error (of the order of 5 to 8 percent) because a pure shear condition does not exist. This error can be decreased by estimating the shear wave velocity from the time interval between arrivals of the waves at the various accelerometers rather than from the time of first arrival at one location.

5.0 SUMMARY

A basic research program combining both experimental and analytical studies has been undertaken to investigate the effects of the 3-D state of stress on the propagation velocity and attenuation of compression and shear waves in soil. Much of the effort in this program for the first year has been directed toward the design and fabrication of the triaxial loading device, a cube, and the associated equipment. The triaxial cube is a metal-walled cube with interior dimensions of 5 ft on a side. Rubber membranes attached to the inside walls are used to apply confining pressures up to 50 psi. Compression and shear waves are excited in the soil by impulses applied at excitation ports which have been constructed in the center of each wall and through which mechanical coupling is made between the soil in the cube and mechanical exciters outside the cube.

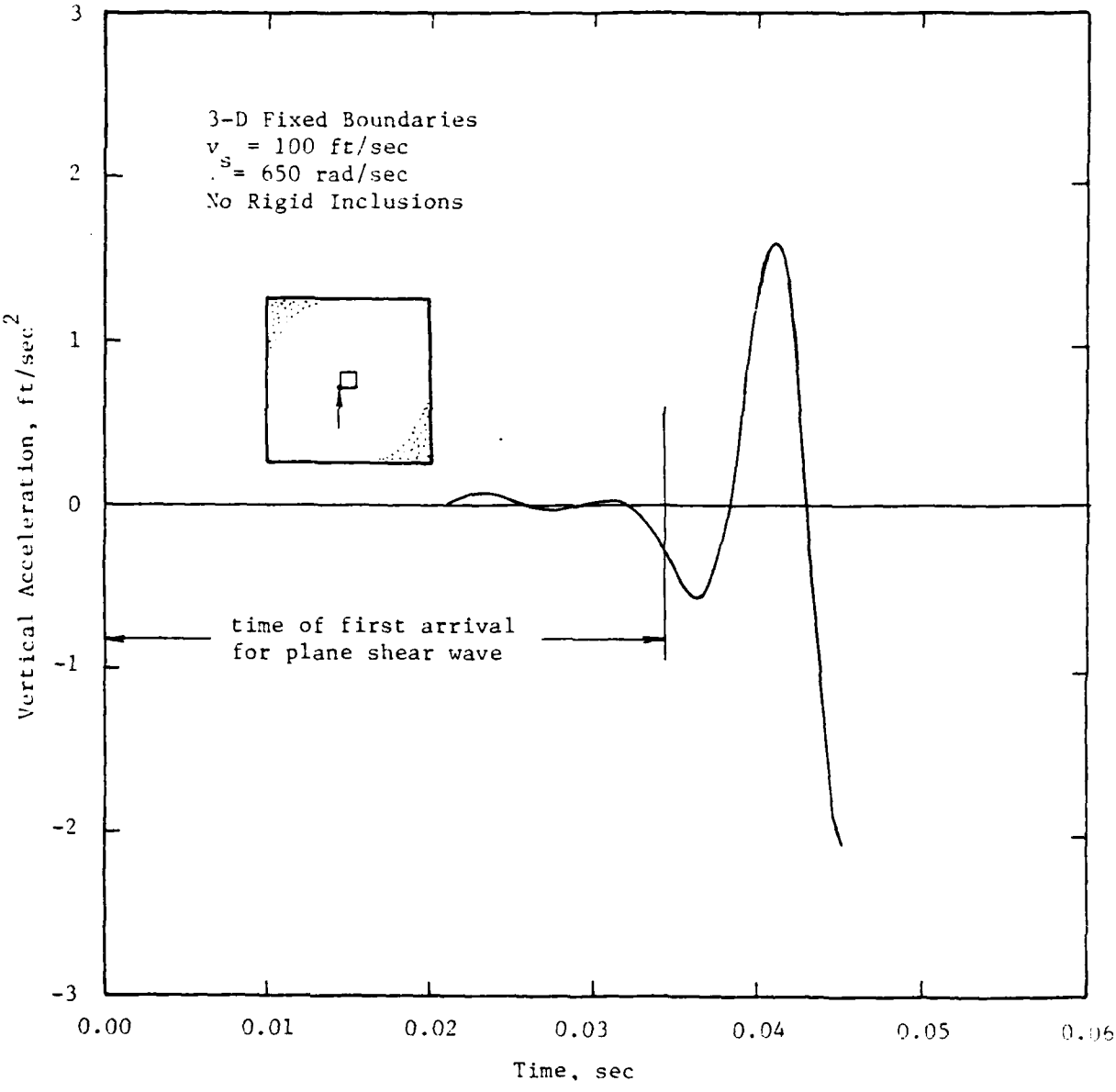

Fig. 29 - Acceleration-Time History of Left Corner of Soil Element in a Sand Mass Without Rigid Inclusions for 3-D Analysis

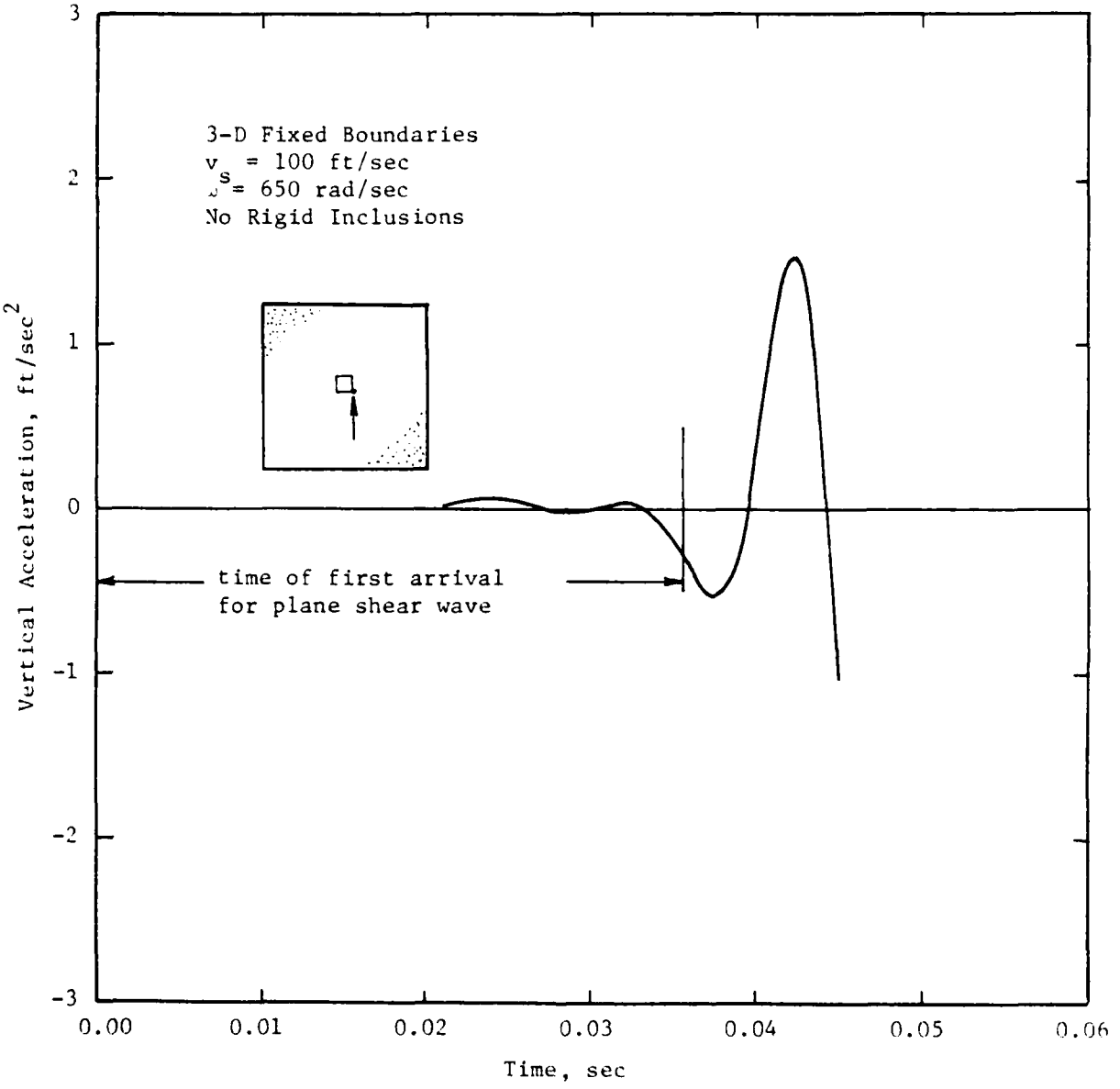

Fig. 30 - Acceleration-Time History of Right Corner of Soil Element in a Sand Mass Without Rigid Inclusion for 3-D Analysis

As of 30 September 1980, the cube is approximately 95 percent completed and all of the associated equipment has either been purchased or designed and fabricated. Dry sand will be used as the soil medium in the initial wave propagation testing. The dynamic properties of this sand under hydrostatic loading conditions have been determined using resonant column equipment to facilitate comparison with results determined in the triaxial cube.

Analytical studies with 2-D and 3-D finite element formulations have been performed to determine the effect of 3-D accelerometers embedded in the soil on the characteristics of compression and shear waves propagating through the soil. These studies indicate that none of the basic characteristics of the waves of importance to this study are significantly affected by these inclusions over the range of wavelengths of interest.

6.0 REFERENCES

1. Beiganousky, W. A. and Marcusson, W. F. III (1976), "Uniform Placement of Sand," Journal of the Geotechnical Engineering Division, ASCE, Vol. 102, No. GT3, March, pp. 229-233.

2. Hardin, B. O. (1978), "The Nature of Stress-Strain Behavior in Soils," Proceedings of the Earthquake Engineering and Soil Dynamics Conference, ASCE, Pasadena, CA, June, Vol. I, pp. 3-90.

3. Hardin, B. O. and Drnevich, V. P. (1972a), "Shear Modulus and Damping in Soils: Measurement and Parameter Effects," Journal of the Soil Mechanics and Foundations Division, ASCE, Vol. 98, No. SM6, June, pp. 603-624.

4. Hardin, B. O. and Drnevich, V. P. (1972b), "Shear Modulus and Damping in Soils: Design Equations and Curves," Journal of the Soil Mechanics and Foundations Division, ASCE, Vol. 98, No. SM7, July, pp. 667-692.

5. Kolbuszswski, J. J. (1948), "General Investigation of the Fundamental Factors Controlling Loose Packing of Sands," Proceedings of the Second International Conference on Soil Mechanics, Rotterdam, Vol. 7, pp. 47-49.

6. Marcusson, W. F. III and Breganousky, W. A. (1977), "Laboratory Standard Penetration Tests on Fine Sands," Journal of the Geotechnical Engineering Division, ASCE, Vol. 103, No. GT6, June, pp. 565-588.